Polynomial graph filter of multiple shifts and distributed implementation of inverse filtering

Nazar Emirov, Cheng Cheng, Junzheng Jiang *Member IEEE*, and Qiyu Sun

***Abstract*—Polynomial graph filters and their inverses play important roles in graph signal processing. An advantage of polynomial graph filters is that they can be implemented in a distributed manner, which involves data transmission between adjacent vertices only. The challenge arisen in the inverse filtering is that a direct implementation may suffer from high computational burden, as the inverse graph filter usually has full bandwidth even if the original filter has small bandwidth. In this paper, we consider distributed implementation of the inverse filtering procedure for a polynomial graph filter of multiple shifts, and we propose two iterative approximation algorithms that can be implemented in a distributed network, where each vertex is equipped with systems for limited data storage, computation power and data exchanging facility to its adjacent vertices. We also demonstrate the effectiveness of the proposed iterative approximation algorithms to implement the inverse filtering procedure and their satisfactory performance to denoise time-varying graph signals and a data set of US hourly temperature at 218 locations.**

Keywords: Graph signal processing, polynomial graph filter, inverse filtering, distributed algorithm, distributed network, Chebyshev polynomial approximation.

I. Introduction

Graph signal processing provides an innovative framework to handle data residing on spatially distributed sensor networks, smart grids, neural networks, social networks and many other irregular domains [1]–[3]. The graph topology in the underlying framework offers a flexible tool to model the interrelationship between data elements. For instance, an edge between two vertices may indicate the correlation between temperature records of neighboring locations, the availability of a direct data exchanging channel between sensors, or the functional connectivity between neural regions in brain. By leveraging graph spectral theory and applied harmonic analysis, graph signal processing has been extensively exploited, and many important concepts in classical signal processing have been extended to graph signal processing [1]–[9].

Let $\mathcal{G} := (V, E)$ be an undirected graph with vertex set $V = \{1, \ldots, N\}$ and edge set $E \subset V \times V$. A *graph filter* $\mathbf{H}$ on the graph $\mathcal{G}$ maps one graph signal $\mathbf{x} = (x(i))_{i\in V}$ to another graph signal $\mathbf{y} = \mathbf{H}\mathbf{x}$ linearly, and it is usually represented by a matrix

$$\mathbf{H} = (H(i,j))_{i,j\in V}. \tag{I.1}$$

Graph filters and their implementations are fundamental in graph signal processing, and they have been used in denoising, smoothing, consensus of multi-agent systems, the estimation of time series and many other applications [10]–[13]. In the classical signal processing, filters are categorized into two families, finite impulse response (FIR) filters and infinite impulse response (IIR) filters. The above concepts on filters have been extended to graph filters with the duration of an FIR filter being replaced by the bandwidth of a graph filter. Here the *bandwidth* $K(\mathbf{H})$ of a graph filter $\mathbf{H} = (H(i,j))_{i,j\in V}$ is the smallest nonnegative integer K such that

$$H(i,j) = 0 \text{ hold for all } i,j \in V \text{ with } \rho(i,j) > K, \tag{I.2}$$

where $\rho(i,j)$ is the geodesic distance between vertices $i,j \in V$ in a connected component of the graph $\mathcal{G}$, and $\rho(i,j) = \infty$ if vertices $i,j \in V$ belong to different connected components [9], [14]. An advantage of a graph filter $\mathbf{H} = (H(i,j))_{i,j\in V}$ with small bandwidth is on the implementation of its filtering procedure $\mathbf{x} \longmapsto \mathbf{y} = \mathbf{H}\mathbf{x}$. One may verify that for an input graph signal $\mathbf{x} = (x(i))_{i\in V}$, the signal value $y(i)$ of the output signal $\mathbf{y} = (y(i))_{i\in V}$ at each vertex $i \in V$ is a "weighted" sum of input signal values at its neighboring vertices $j \in V$,

$$y(i) = \sum_{\rho(i,j)\le K(\mathbf{H})} H(i,j)x(j), \ i \in V. \tag{I.3}$$

The above distributed implementation of the filtering procedure in the vertex domain provides an indispensable tool for data processing on a graph of large order, as a centralized implementation may suffer from high computational burden [12], [15].

An elementary graph filter is the *graph shift*, which has bandwidth at most one. Illustrative examples of graph shifts on a graph $\mathcal{G}$ are the adjacency matrix $\mathbf{A}_\mathcal{G}$, Laplacian matrix $\mathbf{L}_\mathcal{G} := \mathbf{D}_\mathcal{G} - \mathbf{A}_\mathcal{G}$, normalized Laplacian matrix $\mathbf{L}_\mathcal{G}^{\rm sym} = \mathbf{D}_\mathcal{G}^{-1/2}\mathbf{L}_\mathcal{G}\mathbf{D}_\mathcal{G}^{-1/2}$ and their variants [6], [12], [17], [18]. The concept of graph shifts plays the similar role in graph signal processing as the one-order delay z^{-1} in classical signal processing. Using commutative graph shifts $\mathbf{S}_1, \ldots, \mathbf{S}_d$, i.e.,

$$\mathbf{S}_k\mathbf{S}_{k'} = \mathbf{S}_{k'}\mathbf{S}_k, \ 1 \le k, k' \le d, \tag{I.4}$$

as building blocks, we may design polynomial graph filters

$$\mathbf{H} = h(\mathbf{S}_1, \ldots, \mathbf{S}_d) = \sum_{l_1=0}^{L_1} \cdots \sum_{l_d=0}^{L_d} h_{l_1,\ldots,l_d}\mathbf{S}_1^{l_1}\cdots\mathbf{S}_d^{l_d} \tag{I.5}$$

to possess certain spectral characteristic, where $h(t_1, \cdots, t_d)$ is a multivariate polynomial

$$h(t_1, \ldots, t_d) = \sum_{l_1=0}^{L_1} \cdots \sum_{l_d=0}^{L_d} h_{l_1,\ldots,l_d} t_1^{l_1} \ldots t_d^{l_d}.$$

Polynomial graph filters $\mathbf{H}$ of the form (I.5) have bandwidth at most $\sum_{k=1}^d L_k$ and hence as shown in (I.3) the corresponding

Nazar and Sun is with Department of Mathematics, University of Central Florida, Orlando, Florida 32816, USA; Cheng is with Department of Mathematics, Duke University, Durham, NC 27708, USA; Jiang is with School of Information and Communication, Guilin University of Electronic Technology, Guilin 541004, China. Emails: nazaremirov@knights.ucf.edu; cheng87@math.duke.edu; jzjiang@guet.edu.cn; qiyu.sun@ucf.edu. This work is partially supported by the National Natural Science Foundation of China (Grant No. 61761011) and the National Science Foundation (DMS-1816313).

filtering procedure can be "locally" implemented in the vertex domain [4], [6], [7], [12], [14], [19].

In the classical signal processing, IIR filters can be designed to provide better spectral characteristic than FIR filters of the same order do, and the corresponding filtering procedures can be implemented by the combination of an FIR filtering and an inverse FIR filtering. Inverse filtering plays an important role in graph signal processing, such as denoising, graph semi-supervised learning, non-subsampled filter banks and signal reconstruction [12], [14], [15], [20]–[22]. The challenge arisen in the inverse filtering is on its implementation, as the inverse filter usually has full bandwidth even if the original filter has small bandwidth.

In this paper, we consider the inverse filtering procedure of a polynomial graph filter of multiple shifts, and we propose two exponentially convergent iterative algorithms to implement the inverse filtering procedure with steps in each iteration involving data exchanging between adjacent vertices only. Therefore the proposed iterative algorithms can be implemented in a distributed network, where each vertex is equipped with systems for limited data storage, computation power and data exchanging facility to its adjacent vertices.

A. Main contributions and related works

Graph signals, such as video and data collected by a sensor network over a period of time, carry different correlation characteristics for different dimensions/directions [2], [3], [23]. Therefore graph filters to process time-varying signals should be designed to reflect spectral characteristic on the vertex domain and also on the temporal domain, and polynomial graph filters of multiple shifts are preferable. Our consideration of polynomial graph filters of multiple shifts is also motivated by directional frequency analysis in [23] and graph filtering in [24] for time-varying graph signal with stationary interactions between nodes in time. A polynomial filter has its bandwidth no larger than the polynomial degree L and then by (I.3) the corresponding filtering procedure can be implemented in a distributed manner that each vertex exchanges data with its *neighboring* vertices within geodesic distance no more than L. For polynomial graph filters of one shift, algorithms have been proposed to implement their filtering procedure in finite steps, with each step including data exchanging between *adjacent* vertices only [10]–[12], [22], [25], [26]. The first main contribution of this paper is the extension of the above distributed implementation to polynomial graph filters of multiple shifts, see Section III.

For a graph filter $\mathbf{H}$ of small bandwidth, the matrix $\mathbf{H}^{-1}$ associated with the inverse filtering procedure usually has full bandwidth. For the case that the filter $\mathbf{H}$ has its eigenvalues contained in the positive axis, the inverse filtering procedure $\mathbf{b} \longmapsto \mathbf{H}^{-1}\mathbf{b}$ can be implemented by applying the gradient descent method,

$$\mathbf{x}^{(m)} = \mathbf{x}^{(m-1)} - \gamma(\mathbf{H}\mathbf{x}^{(m-1)} - \mathbf{b}),\ m \ge 1, \tag{I.6}$$

where γ is an appropriate step length [25], [27], [28]. To consider implementation of inverse filtering of an arbitrary invertible filter $\mathbf{H}$ of small bandwidth, we start from selecting a graph filter $\mathbf{G}$ with small bandwidth to approximate the inverse filter $\mathbf{H}^{-1}$, and then we propose an iterative approximation algorithm to implement the inverse filtering procedure with each iteration mainly including two filtering procedures associated with filters $\mathbf{H}$ and $\mathbf{G}$. The second main contribution of this paper is to show that the above iterative approximation algorithm converges exponentially, see Theorem IV.1. Moreover, the corresponding iterative approximation algorithm with $\mathbf{G} = \gamma\mathbf{I}$ coincides with the gradient descent method (I.6) with zero initial, see Remark IV.2.

The performance of the proposed iterative algorithm depends on the selection of the approximation filter $\mathbf{G}$ to the inverse filter $\mathbf{H}^{-1}$. The third main contribution of this paper is that for a polynomial graph filter $\mathbf{H}$, we introduce optimal polynomial filters and Chebyshev polynomial filters to approximate the inverse filter $\mathbf{H}^{-1}$, and then each iteration in the corresponding iterative algorithms contains few steps with each step involving data exchanging between adjacent vertices only, see Theorems V.1 and V.3. The effectiveness of these two iterative algorithms to implement the inverse filtering procedure is demonstrated in Section VI. We remark that for polynomial graph filter of one shift, there are several methods to implement the inverse filtering in a distributed manner [12], [15], [17], [22], [25], [26].

B. Organization

In Section II, we introduce two illustrative families of commutative graph shifts on circulant graphs and product graphs. For a polynomial filter of the form (I.5), we propose an iterative algorithm with less than $\prod_{k=1}^{d}(L_k+2)$ steps in Section III to implement the filtering procedure $\mathbf{x} \longmapsto \mathbf{H}\mathbf{x}$, where at every step, the output signal value at each vertex is updated from a linear combination of the input signal values at adjacent vertices. Based on a graph filter approximation $\mathbf{G}$ to the inverse filter $\mathbf{H}^{-1}$, we introduce an exponentially convergent iterative algorithm in Section IV to implement the inverse filtering procedure $\mathbf{b} \longmapsto \mathbf{H}^{-1}\mathbf{b}$, see Theorem IV.1. For an invertible polynomial graph filter $\mathbf{H}$, we introduce optimal polynomial filters $\mathbf{G}_L^*, L \ge 0$, and Chebyshev polynomial filters $\mathbf{G}_K, K \ge 0$, to approximate the inverse filter $\mathbf{H}^{-1}$, and we can use the associated iterative algorithms to implement the inverse filtering procedure $\mathbf{b} \longmapsto \mathbf{H}^{-1}\mathbf{b}$, see Theorems V.1 and V.3. In the first part of Section VI, we demonstrate the implementation of the proposed iterative algorithms for inverse filtering on a circulant graph, and compare their performances with the gradient descent method with zero initial [25] and the autoregressive moving average algorithm [22]. In the second and third parts of Section VI, we apply the proposed iterative algorithms to denoise time-varying signals governed by some differential equations and a US hourly temperature data set respectively. In Appendix A, we give a sufficient condition on graph filters being polynomial of multiple graph shifts.

C. Notation

In this paper, we use boldface uppercase and lowercase characters to represent matrices and vectors respectively, except that we use a boldface uppercase character to represent a time-varying signal and also its vectorization. Denote the identity matrix and zero vector of appropriate sizes by $\mathbf{I}$

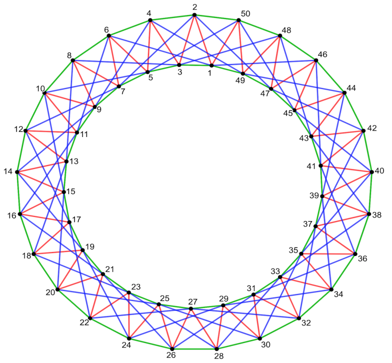

Fig. 1: The circulant graph with 50 nodes and generating set $S = \{1, 2, 5\}$, where edges in red/green/blue are also edges of the cycle graphs $\mathcal{C}_1$, $\mathcal{C}_2$ and $\mathcal{C}_5$ generated by $\{1\}, \{2\}, \{5\}$ respectively.

and $\mathbf{0}$ respectively. For a vector $\mathbf{x} = (x(i))_{i \in V}$ we denote its Euclidean norm and maximal norm by $\|\mathbf{x}\|_2$ and $\|\mathbf{x}\|_\infty$ respectively, and for a matrix $\mathbf{A}$ we denote its trace and operator norm by $\mathrm{tr}(\mathbf{A})$ and $\|\mathbf{A}\|_2 = \sup_{\|\mathbf{x}\|_2=1} \|\mathbf{A}\mathbf{x}\|_2$ respectively. For two matrices $\mathbf{A}$ and $\mathbf{B}$, we denote their Kronecker product by $\mathbf{A} \otimes \mathbf{B}$. For $\mathbf{k} = (k_1, ..., k_d)^T \in \mathbb{Z}_+^d$ we set $|\mathbf{k}| = \sum_{i=1}^d k_i$, and for a set E we use $\#E$ to denote its cardinality.

II. Commutative graph shifts

In this section, we introduce two illustrative families of commutative graph shifts $\mathbf{S}_1, \ldots, \mathbf{S}_d$ on circulant graphs and Cartesian product graphs.

A. Circulant graphs

Let $V = \{1, \ldots, N\}$ and $S = \{S_1, \ldots, S_d\} \subset \{1, \ldots, \lfloor N/2 \rfloor\}$. We define the *circulant* graph $\mathcal{C}(S) = (V, E(S))$ generated by S as

$$(i, j) \in E(S) \text{ if and only if } i - j \in \pm S + N\mathbb{Z}, \tag{II.1}$$

see Figure 1 for the circulant graph with 50 vertices and generating set $S = \{1, 2, 5\}$. A circulant graph $\mathcal{C}(S)$ can be decomposed into a family of cycle graphs $\mathcal{C}(S_k)$ generated by $S_k = \{s_k\}, 1 \le k \le d$, and its normalized Laplacian matrix $\mathbf{L}^{\mathrm{sym}}_{\mathcal{C}(S)}$ is the average of normalized Laplacian matrices $\mathbf{L}^{\mathrm{sym}}_k$ on the cycle graphs $\mathcal{C}(S_k), 1 \le k \le d$, i.e.,

$$\mathbf{L}^{\mathrm{sym}}_{\mathcal{C}(S)} = \frac{1}{d} \sum_{k=1}^d \mathbf{L}^{\mathrm{sym}}_k. \tag{II.2}$$

Observe that

$$\mathbf{L}^{\mathrm{sym}}_k = \mathbf{I} - (\mathbf{L}^{s_k} + \mathbf{L}^{-s_k})/2, \ 1 \le k \le d,$$

where $\mathbf{L}$ is the circulant matrix of size $N \times N$ generated by $(0, 1, 0, \cdots, 0)$. Therefore we have

Proposition II.1. The normalized Laplacian matrices $\mathbf{L}^{\mathrm{sym}}_k$ of the cycle graphs $\mathcal{C}(S_k), 1 \le k \le d$, are commutative graph shifts on the circulant graph $\mathcal{C}(S)$,

$$\mathbf{L}^{\mathrm{sym}}_k \mathbf{L}^{\mathrm{sym}}_{k'} = \mathbf{L}^{\mathrm{sym}}_{k'} \mathbf{L}^{\mathrm{sym}}_k, \ 1 \le k, k' \le d. \tag{II.3}$$

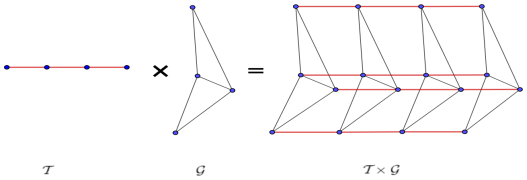

Fig. 2: Cartesian product $\mathcal{T} \times \mathcal{G}$ of a line graph $\mathcal{T}$ and an undirected graph $\mathcal{G}$.

B. Cartesian product graphs and time-varying graph signals

Let $\mathcal{G}_1 = (V_1, E_1)$ and $\mathcal{G}_2 = (V_2, E_2)$ be two finite graphs with adjacency matrices $\mathbf{A}_1$ and $\mathbf{A}_2$. Their Cartesian product graph $\mathcal{G}_1 \times \mathcal{G}_2$ has vertex set $V_1 \times V_2$ and adjacency matrix given by $\mathbf{A} = \mathbf{A}_1 \otimes \mathbf{I}_{\#V_2} + \mathbf{I}_{\#V_1} \otimes \mathbf{A}_2$ [34], [35]. By the mixed-product property

$$(\mathbf{A} \otimes \mathbf{B})(\mathbf{C} \otimes \mathbf{D}) = (\mathbf{AC}) \otimes (\mathbf{BD}) \tag{II.4}$$

for Kronecker product of matrices $\mathbf{A}, \mathbf{B}, \mathbf{C}, \mathbf{D}$ of appropriate sizes [16], we have

Proposition II.2. Let $\mathcal{G}_1 = (V_1, E_1)$ and $\mathcal{G}_2 = (V_2, E_2)$ be two finite graphs with normalized Laplacian matrices $\mathbf{L}^{\mathrm{sym}}_1$ and $\mathbf{L}^{\mathrm{sym}}_2$ respectively. Then $\mathbf{L}^{\mathrm{sym}}_1 \otimes \mathbf{I}_{\#V_2}$ and $\mathbf{I}_{\#V_1} \otimes \mathbf{L}^{\mathrm{sym}}_2$ are commutative graph shifts of the Cartesian product graph $\mathcal{G}_1 \times \mathcal{G}_2$.

A time-varying graph signal $\mathbf{X} = [\mathbf{x}_1, \cdots, \mathbf{x}_M]$ on a graph $\mathcal{G} = (V, E)$ is a time series of graph data $\mathbf{x}_t$ on $\mathcal{G}$ sampled at M successive instants $t_1, \ldots, t_M$. Define a line graph $\mathcal{T} = (T, F)$ with the vertex set $T = \{t_1, \cdots, t_M\}$ and edge set $F = \{(t_1, t_2), \ldots, (t_{M-1}, t_M)\} \cup \{(t_M, t_{M-1}), \ldots, (t_2, t_1)\}$. Then the time-varying graph signal $\mathbf{X}$ is a signal on the Cartesian product graph $\mathcal{T} \times \mathcal{G}$, see Figure 2.

III. Polynomial filters and local implementation

The filtering procedure $\mathbf{x} \longmapsto \mathbf{S}\mathbf{x}$ associated with a graph shift $\mathbf{S} = (S(i, j))_{i,j \in V}$ is a local operation that updates signal value at each vertex $i \in V$ by a "weighted" linear combination of signal values at *adjacent* vertices $j \in \mathcal{N}_i$,

$$\tilde{x}(i) = \sum_{j \in \mathcal{N}_i} S(i, j) x(j),$$

where $\mathbf{x} = (x(i))_{i \in V}$ and $\mathbf{S}\mathbf{x} = (\tilde{x}(i))_{i \in V}$. Here and thereafter for a vertex i in a graph $\mathcal{G} = (V, E)$, we denote the set of its adjacent vertices by $\mathcal{N}_i$. The above local implementation of filtering procedure has been extended to a polynomial graph filter $\mathbf{H} = \sum_{l=0}^L h_l \mathbf{S}^l$ of the shift $\mathbf{S}$,

$$\begin{cases} \mathbf{z}^{(0)} = h_L \mathbf{x}, \\ \mathbf{z}^{(n)} = h_{L-n} \mathbf{x} + \mathbf{S}\mathbf{z}^{(n-1)}, \ n = 1, \ldots, L, \\ \mathbf{H}\mathbf{x} = \mathbf{z}^{(L)}, \end{cases} \tag{III.1}$$

where the filtering procedure $\mathbf{x} \longmapsto \mathbf{H}\mathbf{x}$ is divided into $(L+1)$-steps with the filtering procedure in each step being a local operation [10]–[12], [22], [26]. The block diagram of the above implementation is shown in Figure 3. In this section, we extend the above implementation to a polynomial graph filter $\mathbf{H}$ of the form (I.5).

For $1 \le d' \le d$, we order $(l_1, \ldots, l_{d'})$ with $0 \le l_k \le L_k, 1 \le k \le d'$ lexicographically as

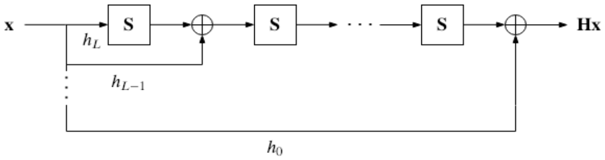

Fig. 3: Local implementation of filtering procedure $\mathbf{x} \longmapsto \mathbf{Hx}$ corresponding to a polynomial graph filter $\mathbf{H} = \sum_{l=0}^{L} h_l \mathbf{S}^l$.

$$m(l_1, \ldots, l_{d'}) = \sum_{k=1}^{d'-1} \Big(\prod_{k'=k+1}^{d'} (L_{k'} + 1) \Big) l_k + l_{d'}, \qquad \text{(III.2)}$$

and we denote the filter coefficients $h_{l_1,\cdots,l_d}$ by $h_{m(l_1,\ldots,l_d)}$. Given an input graph signal $\mathbf{x}$, we first calculate

$$\mathbf{y}^{(d)}_{m(l_1,\cdots,l_{d-1})} = \sum_{l_d=0}^{L_d} h_{m(l_1,\ldots,l_{d-1},l_d)} \mathbf{S}_d^{l_d} \mathbf{x} \qquad \text{(III.3)}$$

for $0 \le l_k \le L_k, 1 \le k \le d-1$. Following the procedure in (III.1), we can obtain the vectors $\mathbf{y}^{(d)}_{m(l_1,\cdots,l_{d-1})}, 0 \le l_k \le L_k, 1 \le k \le d-1$, in (L_d+1)-steps with the filtering procedure in each step being a local operation,

$$\begin{cases} \mathbf{z}^{(0)} = h_{m(l_1,\ldots,l_{d-1},L_d)} \mathbf{x}, \\ \mathbf{z}^{(n)} = h_{m(l_1,\ldots,l_{d-1},L_d-n)} \mathbf{x} + \mathbf{S}_d \mathbf{z}^{(n-1)}, \ n = 1, \ldots, L_d, \\ \mathbf{y}^{(d)}_{m(l_1,\cdots,l_{d-1})} = \mathbf{z}^{(L_d)}. \end{cases} \qquad \text{(III.4)}$$

By (I.5) and (III.3), we have

$$\mathbf{Hx} = \sum_{l_1=0}^{L_1} \cdots \sum_{l_{d-1}=0}^{L_{d-1}} \mathbf{S}_1^{l_1} \cdots \mathbf{S}_{d-1}^{l_{d-1}} \mathbf{y}^{(d)}_{m(l_1,\cdots,l_{d-1})}. \qquad \text{(III.5)}$$

Next we calculate

$$\mathbf{y}^{(d')}_{m(l_1,\cdots,l_{d'-1})} = \sum_{l_{d'}=0}^{L_{d'}} \mathbf{S}_{d'}^{l_{d'}} \mathbf{y}^{(d'+1)}_{m(l_1,\cdots,l_{d'-1},l_{d'})} \qquad \text{(III.6)}$$

by induction on $d' = d-1, \ldots, 2$, where $0 \le l_k \le L_k, 1 \le k \le d'-1$. The vectors $\mathbf{y}^{(d')}_{m(l_1,\cdots,l_{d'-1})}, 0 \le l_k \le L_k, 1 \le k \le d'-1$, can be obtained in $(L_{d'}+1)$-steps with the filtering procedure in each step being a local operation,

$$\begin{cases} \mathbf{z}^{(0)} = \mathbf{y}^{(d'+1)}_{m(l_1,\cdots,l_{d'-1},L_{d'})}, \\ \mathbf{z}^{(n)} = \mathbf{y}^{(d'+1)}_{m(l_1,\cdots,l_{d'-1},L_{d'}-n)} + \mathbf{S}_{d'} \mathbf{z}^{(n-1)}, \ n = 1, \ldots, L_{d'}, \\ \mathbf{y}^{(d')}_{m(l_1,\cdots,l_{d'-1})} = \mathbf{z}^{(L_{d'})}. \end{cases} \qquad \text{(III.7)}$$

By (III.5) and (III.6), we can prove that

$$\mathbf{Hx} = \sum_{l_1=0}^{L_1} \cdots \sum_{l_{d'-1}=0}^{L_{d'-1}} \mathbf{S}_1^{l_1} \cdots \mathbf{S}_{d'-1}^{l_{d'-1}} \mathbf{y}^{(d')}_{m(l_1,\cdots,l_{d'-1})} \qquad \text{(III.8)}$$

by induction on $d' = d, d-1, \ldots, 2$. Taking $d' = 2$ in (III.8), we finally arrive the output of the filtering procedure,

$$\mathbf{Hx} = \sum_{l_1=0}^{L_1} \mathbf{S}_1^{l_1} \mathbf{y}^{(2)}_{m(l_1)}, \qquad \text{(III.9)}$$

which can be obtained in (L_1+1)-steps with the filtering procedure in each step being a local operation:

$$\begin{cases} \mathbf{z}^{(0)} = \mathbf{y}^{(2)}_{m(L_1)}, \\ \mathbf{z}^{(n)} = \mathbf{y}^{(2)}_{m(L_1-n)} + \mathbf{S}_1 \mathbf{z}^{(n-1)}, \ n = 1, \ldots, L_1, \\ \mathbf{Hx} = \mathbf{z}^{(L_1)}. \end{cases} \qquad \text{(III.10)}$$

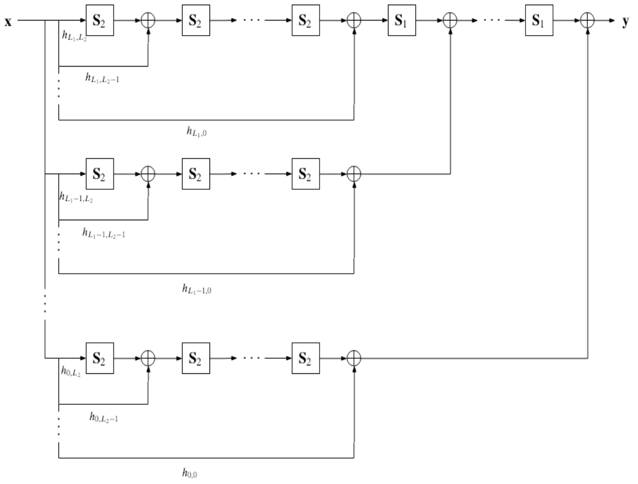

Fig. 4: Local implementation of filtering procedure $\mathbf{x} \longmapsto \mathbf{y} = \mathbf{Hx}$ corresponding to a polynomial graph filter $\mathbf{H} = \sum_{l_1=0}^{L_1} \sum_{l_2=0}^{L_2} h_{l_1,l_2} \mathbf{S}_1^{l_1} \mathbf{S}_2^{l_2}$ of commutative shifts $\mathbf{S}_1$ and $\mathbf{S}_2$.

Algorithm III.1 Local implementation of the filtering procedure $\mathbf{x} \longmapsto \mathbf{y} = \mathbf{Hx}$ for the polynomial filter $\mathbf{H} = \sum_{l_1=0}^{L_1} \sum_{l_2=0}^{L_2} \sum_{l_3=0}^{L_3} h_{l_1,l_2,l_3} \mathbf{S}_1^{l_1} \mathbf{S}_2^{l_2} \mathbf{S}_3^{l_3}$.

```
Inputs: Polynomial coefficients $h_{l_1,l_2,l_3}$ of the polynomial filter $\mathbf{H}$, commutative graph shifts $\mathbf{S}_1, \mathbf{S}_2, \mathbf{S}_3$, and input graph signal $\mathbf{x}$.
1) for $1 \le j \le (L_1+1)(L_2+1)$,
      Set $l_1 = \lfloor (j-1)/(L_2+1) \rfloor$, $l_2 = j-1-(L_2+1)l_1$ and $\mathbf{z} = h_{l_1,l_2,L_3}\mathbf{x}$
      for $l = 1, \ldots, L_3$
         $\mathbf{z} = h_{l_1,l_2,L_3-l}\mathbf{x} + \mathbf{S}_3\mathbf{z}$
      end
      Set $\mathbf{U}(:,j) = \mathbf{z}$
   end
2) for $1 \le i \le L_1+1$,
      Set $\mathbf{w} = \mathbf{U}(:, i(L_2+1))$
      for $l = 1, \ldots, L_2$
         $\mathbf{w} = \mathbf{U}(:, i(L_2+1)-l) + \mathbf{S}_2\mathbf{w}$
      end
      Set $\mathbf{W}(:,i) = \mathbf{w}$
   end
3) Set $\mathbf{u} = \mathbf{W}(:, L_1+1)$
      for $l = 1, \ldots, L_1$
         $\mathbf{u} = \mathbf{W}(:, L_1+1-l) + \mathbf{S}_1\mathbf{u}$
      end
Output: $\mathbf{y} = \mathbf{u}$
```

The block diagram for the proposed implementation (III.4), (III.7) and (III.10) with $d = 2$ is presented in Figure 4. The algorithm of the proposed implementation for $d = 3$ in a matrix form is shown in Algorithm III.1, where $\mathbf{U} = (\mathbf{U}(:,j))_{1 \le j \le (L_1+1)(L_2+1)}$ has columns $\mathbf{y}^{(3)}_{(L_2+1)l_1+l_2}, 0 \le l_1 \le L_1, 0 \le l_2 \le L_2$, and $\mathbf{W} = (\mathbf{W}(:,i))_{1 \le i \le L_1+1}$ has columns $\mathbf{y}^{(2)}_{l_1}, 0 \le l_1 \le L_1$, respectively.

Remark III.1. The proposed algorithm (III.4), (III.7) and (III.10) can be implemented in a distributed network, where each vertex is equipped with systems for limited data storage, computation power and data exchanging facility to its adjacent vertices. We can verify that the distributed implementation of the proposed algorithm (III.4), (III.7) and (III.10) requires the computation subsystem at a vertex $i \in V$ to perform about $O\big((L_1+1)\cdots(L_d+1)\#\mathcal{N}_i\big)$ additions and multiplications, the communication subsystem to exchange its i-th and adjacent j-th components of the original graph signal $\mathbf{x}$ and outputs of filtering procedure at different steps about $O\big((L_1+1)\ldots(L_d+1)\#\mathcal{N}_i\big)$ times, and the memory subsystem to store data of size $O\big((L_1+1)\ldots(L_d+1)\#\mathcal{N}_i\big)$, including polynomial coefficients of the polynomial filter $\mathbf{H}$, the i-th row of graph shifts $\mathbf{S}_1,\ldots,\mathbf{S}_d$, and the i-th and its adjacent j-th components of the original graph signal $\mathbf{x}$ and outputs of the filtering procedure at different steps, where $j \in \mathcal{N}_i$.

Remark III.2. Denote the order and degree of the graph $\mathcal{G}$ by $N = \#V$ and $\deg\mathcal{G}$ respectively. Observe that the proposed implementation (III.4), (III.7) and (III.10) contains less than $\prod_{k=1}^d (L_k+2)$ steps with the filtering procedure in each step being a local operation. Then the proposed implementation for the filtering procedure $\mathbf{x} \longmapsto \mathbf{H}\mathbf{x}$ can be also implemented in a centralized facility, which requires to perform $O\big(N\big(\prod_{k=1}^d (L_k+1)\big)\deg\mathcal{G}\big)$ additions and multiplications, and to have memory of size about $O\big(N\big(\prod_{k=1}^d (L_k+1)\big)\deg\mathcal{G}\big)$ to store the graph shifts $\mathbf{S}_1,\ldots,\mathbf{S}_d$, the polynomial coefficients of the polynomial filter $\mathbf{H}$, the original graph signal and outputs of the filtering procedure at different steps.

IV. Inverse Filtering and Iterative Approximation Algorithm

In some applications, such as signal denoising, inpainting, smoothing, reconstructing and semi-supervised learning [12], [14], [21], [22], [27], an inverse filtering procedure

$$\mathbf{x} = \mathbf{H}^{-1}\mathbf{b} \tag{IV.1}$$

is involved. In this section, we introduce an exponentially convergent iterative algorithm to implement the inverse filtering procedure (IV.1) with each iteration being implemented by some filtering procedures.

Let $\mathbf{G}$ be an approximation graph filter to the inverse filter $\mathbf{H}^{-1}$ such that the spectrum of $\mathbf{HG}$ is contained in a disk with center one and radius $\epsilon \in [0,1)$, i.e.,

$$\sigma(\mathbf{HG}) \subset \{z:\ |z-1| \le \epsilon\}. \tag{IV.2}$$

An equivalent condition to the above requirement is that the spectral radius of $\mathbf{I}-\mathbf{HG}$ is strictly less than 1,

$$\lim_{n\to\infty} \|(\mathbf{I}-\mathbf{HG})^n\|_2^{1/n} \le \epsilon < 1. \tag{IV.3}$$

By (IV.3), we can rewrite (IV.1) as

$$\mathbf{x} = \mathbf{G}(\mathbf{HG})^{-1}\mathbf{b} = \mathbf{G}\sum_{k=0}^{\infty}(\mathbf{I}-\mathbf{HG})^k\mathbf{b}. \tag{IV.4}$$

Based on the above representation, we propose the following iterative algorithm for the inverse filtering procedure (IV.1):

$$\begin{cases} \mathbf{z}^{(m)} = \mathbf{G}\mathbf{b}^{(m-1)}, \\ \mathbf{b}^{(m)} = \mathbf{b}^{(m-1)} - \mathbf{H}\mathbf{z}^{(m)}, \\ \mathbf{x}^{(m)} = \mathbf{x}^{(m-1)} + \mathbf{z}^{(m)},\ m \ge 1, \end{cases} \tag{IV.5}$$

with initials

$$\mathbf{b}^{(0)} = \mathbf{b} \ \text{ and } \ \mathbf{x}^{(0)} = \mathbf{0}. \tag{IV.6}$$

Due to the approximation property of the graph filter $\mathbf{G}$ to the inverse filter $\mathbf{H}^{-1}$, we call the above algorithm as an *iterative approximation algorithm*. By (IV.5) and (IV.6), we can prove by induction on m that

$$\mathbf{b}^{(m)} = (\mathbf{I}-\mathbf{HG})^m\mathbf{b} \tag{IV.7}$$

and

$$\mathbf{x}^{(m)} = \sum_{n=0}^{m-1}\mathbf{G}\mathbf{b}^{(n)} = \mathbf{G}\sum_{n=0}^{m-1}(\mathbf{I}-\mathbf{HG})^n\mathbf{b},\ m \ge 1. \tag{IV.8}$$

By (IV.2), (IV.4) and (IV.8), we have

$$\|\mathbf{x}^{(m)}-\mathbf{x}\|_2 \le \|\mathbf{G}\|_2\|\mathbf{H}\|_2\Big(\sum_{n=m}^{\infty}\|(\mathbf{I}-\mathbf{HG})^n\|_2\Big)\|\mathbf{x}\|_2, m \ge 1. \tag{IV.9}$$

Therefore we conclude from (IV.3) and (IV.9) that the iterative approximation algorithm (IV.5) and (IV.6) converges exponentially.

Theorem IV.1. Let $\mathbf{b}$ be a graph signal and $\mathbf{H}$ be a graph filter. Take a graph filter $\mathbf{G}$ such that (IV.2) holds for some $\epsilon \in [0,1)$. Then $\mathbf{x}^{(m)}, m \ge 1$, in the iterative approximation algorithm (IV.5) and (IV.6) converges exponentially to $\mathbf{H}^{-1}\mathbf{b}$. Moreover, for any $r \in (\epsilon, 1)$, there exists a positive constant C such that

$$\|\mathbf{x}^{(m)} - \mathbf{H}^{-1}\mathbf{b}\|_2 \le C\|\mathbf{x}\|_2 r^m,\ m \ge 1. \tag{IV.10}$$

By Theorem IV.1, the inverse filtering procedure (IV.1) can be implemented by applying the iterative approximation algorithm (IV.5) and (IV.6) with the graph filter $\mathbf{G}$ being chosen so that (IV.2) holds.

We finish this section with two remarks on the comparison among the gradient descent method [25], the autoregressive moving average (ARMA) method [22], and the proposed iterative approximation algorithm (IV.5) and (IV.6).

Remark IV.2. For the case that the graph filter $\mathbf{H}$ has its spectrum contained in the positive axis, the inverse filtering procedure (IV.1) can be implemented by the gradient descent method (I.6), where γ is an appropriate step length. The above iterative method is shown in [25] to be convergent when $0 < \gamma < 2/\alpha_2$ and to have fastest convergence when $\gamma = 2/(\alpha_1+\alpha_2)$, where α_1 and α_2 are the minimal and maximal eigenvalues of the matrix $\mathbf{H}$. By (I.6), we have that

$$\mathbf{x}^{(m)} = \gamma\sum_{k=0}^{m-1}(\mathbf{I}-\gamma\mathbf{H})^k\mathbf{b} + (\mathbf{I}-\gamma\mathbf{H})^m\mathbf{x}^{(0)},\ m \ge 1. \tag{IV.11}$$

By (IV.8) and (IV.11), the sequence $\mathbf{x}^{(m)}, m \ge 1$, in the gradient descent algorithm with zero initial coincides with the sequence in the iterative approximation algorithm (IV.5) and (IV.6) with $\mathbf{G} = \gamma\mathbf{I}$, in which the requirement (IV.2) is met as $\sigma(\mathbf{HG}) = \gamma\sigma(\mathbf{H}) \subset \gamma[\alpha_1, \alpha_2] \subset (0,2)$ whenever $0 < \gamma < 2/\alpha_2$.

Remark IV.3. Let $\mathbf{S}$ be a graph shift and $\mathbf{H} = h(\mathbf{S})$ be a polynomial graph filter with roots of the polynomial h being simple and outside the disk $B(0, \|\mathbf{S}\|_2) = \{z \in \mathbb{C}, |z| \le \|\mathbf{S}\|_2\}$. Write $(h(t))^{-1} = \sum_{k=1}^L a_k(1-b_kt)^{-1}$ for some coefficients a_k, b_k satisfying

$$|b_k|\|\mathbf{S}\|_2 < 1,\ 1 \le k \le L. \tag{IV.12}$$

Then we can decompose the inverse filter $\mathbf{H}^{-1}$ into a family of elementary inverse filters $(\mathbf{I}-b_k\mathbf{S})^{-1}$,

$$\mathbf{H}^{-1}=\sum_{k=1}^{L} a_k(\mathbf{I}-b_k\mathbf{S})^{-1}. \tag{IV.13}$$

Due to the above decomposition, the inverse filtering procedure (IV.1) can be implemented as follows,

$$\mathbf{x}=\sum_{k=1}^{L} a_k(\mathbf{I}-b_k\mathbf{S})^{-1}\mathbf{b}=:\sum_{k=1}^{L} a_k\mathbf{x}_k. \tag{IV.14}$$

The autoregressive moving average (ARMA) method in [22] uses the above approach with the elementary inverse procedure $\mathbf{x}_k=(\mathbf{I}-b_k\mathbf{S})^{-1}\mathbf{b}$ implemented by the following iterative approach,

$$\mathbf{x}_k^{(m)}=b_k\mathbf{S}\mathbf{x}_k^{(m-1)}+\mathbf{b},\ m\ge 1 \tag{IV.15}$$

with initial $\mathbf{x}_k^{(0)}=\mathbf{0}$. We remark that the above approach is the same as the iterative approximation algorithm (IV.5) and (IV.6) with $\mathbf{H}$ and $\mathbf{G}$ replaced by $\mathbf{I}-b_k\mathbf{S}$ and $\mathbf{G}=\mathbf{I}$ respectively, $\mathbf{x}_k^{(m)}=\mathbf{x}_k^{(m-1)}+\mathbf{b}_k^{(m-1)}$ and $\mathbf{b}_k^{(m)}=b_k\mathbf{S}\mathbf{b}_k^{(m-1)},\ m\ge 1$. Moreover, in the above selection of the graph filters $\mathbf{H}$ and $\mathbf{G}$, the requirement (IV.2) is met as

$$\|\mathbf{I}-\mathbf{H}\mathbf{G}\|_2\le |b_k|\|\mathbf{S}\|_2<1,\ 1\le k\le L.$$

V. Iterative Polynomial Approximation Algorithms

The performance of the iterative approximation algorithm (IV.5) and (IV.6) depends on the selection of the approximation filter $\mathbf{G}$ to the inverse filter $\mathbf{H}^{-1}$. In this section, we consider the inverse filtering of a polynomial graph filter $\mathbf{H}$ of commutative shifts $\mathbf{S}_1,...,\mathbf{S}_d$, and we apply the proposed algorithm (IV.5) and (IV.6) to implement the inverse filtering procedure (IV.1), with the filter $\mathbf{G}$ being a polynomial graph filter with small bandwidth. The advantage of the above selection of the graph filter $\mathbf{G}$ is that as proposed in Section III, the iterative algorithm (IV.5) and (IV.6) can be locally implemented in each iteration in a distributed network.

A. Polynomial interpolation and optimal polynomial approximation

Due to the communtativity of graph shifts $\mathbf{S}_1,...,\mathbf{S}_d$, they can be upper-triangularized simultaneously by [36, Theorem 2.3.3], i.e.,

$$\hat{\mathbf{S}}_k=\mathbf{U}^*\mathbf{S}_k\mathbf{U},\ 1\le k\le d, \tag{V.1}$$

are upper triangular matrices for some unitary matrix $\mathbf{U}$. Set $\hat{\mathbf{S}}_k=(\hat{S}_k(i,j))_{1\le i,j\le N}, 1\le k\le d$ and

$$\Lambda=\big\{\boldsymbol{\lambda}_i=\big(\hat{S}_1(i,i),...,\hat{S}_d(i,i)\big),1\le i\le N\big\}, \tag{V.2}$$

where $N=\#V$ is the order of the graph $\mathcal{G}=(V,E)$. As $\hat{S}_k(i,i), 1\le i\le N$, are eigenvalues of $\mathbf{S}_k,\ 1\le k\le d$, we call Λ as the *joint spectrum* of $\mathbf{S}_1,\dots,\mathbf{S}_d$. For polynomial filters $\mathbf{H}=h(\mathbf{S}_1,\dots,\mathbf{S}_d)$ and $\mathbf{G}=g(\mathbf{S}_1,\dots,\mathbf{S}_d)$, one may verify that $\mathbf{U}^*\mathbf{H}\mathbf{G}\mathbf{U}$ is an upper triangular matrix with diagonal entries $h(\boldsymbol{\lambda}_i)g(\boldsymbol{\lambda}_i),\ \boldsymbol{\lambda}_i\in\Lambda$. Consequently, the requirement (IV.2) for the polynomial graph filter $\mathbf{G}$ becomes

$$\epsilon:=\sup_{\boldsymbol{\lambda}_i\in\Lambda}\big|1-h(\boldsymbol{\lambda}_i)g(\boldsymbol{\lambda}_i)\big|<1. \tag{V.3}$$

A necessary condition for the existence of a polynomial g such that (V.3) holds is that

$$h(\boldsymbol{\lambda}_i)\ne 0 \text{ for all } \ \boldsymbol{\lambda}_i\in\Lambda, \tag{V.4}$$

or equivalently the filter $\mathbf{H}=h(\mathbf{S}_1,...,\mathbf{S}_d)$ is represented by a nonsingular matrix. Conversely if (V.4) holds, $(\boldsymbol{\lambda}_i,1/h(\boldsymbol{\lambda}_i)), 1\le i\le N$, can be interpolated by a polynomial g_I of degree at most $N+1$ [38], i.e.,

$$g_I(\boldsymbol{\lambda}_i)=1/h(\boldsymbol{\lambda}_i),\ \boldsymbol{\lambda}_i\in\Lambda. \tag{V.5}$$

For the above polynomial g_I, we have that

$$\epsilon=\max_{\boldsymbol{\lambda}_i\in\Lambda}|1-h(\boldsymbol{\lambda}_i)g_I(\boldsymbol{\lambda}_i)|=0.$$

Take $\mathbf{G}_I=g_I(\mathbf{S}_1,\dots,\mathbf{S}_d)$. Then all eigenvalues of $\mathbf{I}-\mathbf{G}_I\mathbf{H}$ are zero and hence the iterative approximation algorithm (IV.5) and (IV.6) converges in at most N steps. We remark that the matrix $\mathbf{I}-\mathbf{G}_I\mathbf{H}$ is not necessarily the zero matrix, or equivalently $\mathbf{G}_I=\mathbf{H}^{-1}$, in general. However, the conclusion $\mathbf{G}_I=\mathbf{H}^{-1}$ holds when all elements $\boldsymbol{\lambda}_i, 1\le i\le N$, in the joint spectrum Λ are distinct. The above conclusion can be proved by following the argument used in the proof of Theorem A.1 in the appendix and the observation that the matrix $\mathbf{I}-\mathbf{G}_I\mathbf{H}$ has all eigenvalues being zero and it commutes with $\mathbf{S}_k, 1\le k\le d$.

For $L\ge 0$, denote the set of all polynomials of degree at most L by $\mathcal{P}_L$. In practice, we may not use the interpolation polynomial g_I in (V.5), and hence the polynomial filter $\mathbf{G}=g_I(\mathbf{S}_1,\dots,\mathbf{S}_d)$ in the iterative approximation algorithm (IV.5) and (IV.6), as it is of high degree in general. By (V.3) and (IV.10), the convergence rate of the iterative approximation algorithm (IV.5) and (IV.6) depends on the quantity ϵ in (V.3). Due to the above observation, we propose to select $g_L^*\in\mathcal{P}_L$ such that

$$g_L^*=\arg\min_{g\in\mathcal{P}_L}\sup_{\boldsymbol{\lambda}_i\in\Lambda}|1-g(\boldsymbol{\lambda}_i)h(\boldsymbol{\lambda}_i)|. \tag{V.6}$$

For a polynomial $g\in\mathcal{P}_L$, we write $g(\mathbf{t})=\sum_{|\mathbf{k}|\le L}c_{\mathbf{k}}\mathbf{t}^{\mathbf{k}}$. Then for the case that all eigenvalues of $\mathbf{S}_k, 1\le k\le d$, are real, i.e., $\Lambda\subset\mathbb{R}^d$, the minimization problem (V.6) can be reformulated as a linear programming,

$$\min\ s\ \text{ subject to }\ -(s-1)\mathbf{1}\le\mathbf{A}\mathbf{c}\le(s+1)\mathbf{1}, \tag{V.7}$$

where $\mathbf{A}=(h(\boldsymbol{\lambda}_i)\boldsymbol{\lambda}_i^{\mathbf{k}})_{1\le i\le N,|\mathbf{k}|\le L}$, $\mathbf{c}=(c_{\mathbf{k}})_{|\mathbf{k}|\le L}$ and $\mathbf{1}$ is the vector with all entries taking value 1. For the polynomial g_L^* constructed in (V.6), we set

$$\mathbf{G}_L^*=g_L^*(\mathbf{S}_1,\dots,\mathbf{S}_d) \tag{V.8}$$

and call the iterative approximation algorithm (IV.5) and (IV.6) with the graph filter $\mathbf{G}$ replaced by $\mathbf{G}_L^*$ by the *iterative optimal polynomial approximation algorithm*, or IOPA in abbreviation,

$$\begin{cases}\mathbf{z}^{(m)}=\mathbf{G}_L^*\mathbf{b}^{(m-1)}\\ \mathbf{b}^{(m)}=\mathbf{b}^{(m-1)}-\mathbf{H}\mathbf{z}^{(m)}\\ \mathbf{x}^{(m)}=\mathbf{x}^{(m-1)}+\mathbf{z}^{(m)},\ m\ge 1,\end{cases} \tag{V.9}$$

where $\mathbf{b}^{(0)}$ and $\mathbf{x}^{(0)}$ are given in (IV.6). Then as proposed in Section III, each iteration in the IOPA algorithm (V.9) can be implemented in finite steps with each step containing data exchanging among adjacent vertices only. By Theorem IV.1, the IOPA algorithm (V.9) converges exponentially when L is so chosen that

$$a_L^*:=\sup_{\boldsymbol{\lambda}_i\in\Lambda}|1-g_L^*(\boldsymbol{\lambda}_i)h(\boldsymbol{\lambda}_i)|<1. \tag{V.10}$$

Theorem V.1. Let $\mathbf{b}$ be a graph signal, $\mathbf{S}_1, ..., \mathbf{S}_d$ be commutative graph shifts, $\mathbf{H}$ be a polynomial graph filter of graph shifts $\mathbf{S}_1, \ldots, \mathbf{S}_d$, and let degree $L \geq 0$ be so chosen that (V.10) holds. Then $\mathbf{x}^{(m)}, m \geq 1$, in the IOPA algorithm (V.9) converges exponentially to $\mathbf{H}^{-1}\mathbf{b}$. Moreover, for any $r \in (a_L^*, 1)$, there exists a positive constant C such that

$$\|\mathbf{x}^{(m)} - \mathbf{H}^{-1}\mathbf{b}\|_2 \leq C\|\mathbf{x}\|_2 r^m, \ m \geq 1. \tag{V.11}$$

Remark V.2. For the case that the graph filter $\mathbf{H}$ has its spectrum contained in $[\alpha_1, \alpha_2]$, the solution of the minimization problem (V.6) with $L = 0$ is given by $g_0^* = 2/(\alpha_1 + \alpha_2)$, where $\alpha_1 = \min_{\boldsymbol{\lambda}_i \in \Lambda} h(\boldsymbol{\lambda}_i)$ and $\alpha_2 = \max_{\boldsymbol{\lambda}_i \in \Lambda} h(\boldsymbol{\lambda}_i)$ are the minimal and maximal eigenvalues of $\mathbf{H}$ respectively. Therefore to implement the inverse filtering procedure (IV.1), the gradient descent method (I.6) with zero initial and step length $\gamma = 2/(\alpha_1 + \alpha_2)$ is the same as the proposed IOPA algorithm (V.9) with $L = 0$, cf. Remark IV.2.

B. Chebyshev approximation

The construction of the interpolating polynomial g_I in (V.5) and the optimal polynomial $g_L^* \in \mathcal{P}_L$ of degree L in (V.6) depends on the prior information of the joint spectrum Λ of commutative graph shifts $\mathbf{S}_k, 1 \leq k \leq d$. However, for a graph $\mathcal{G}$ of large order, it is often computationally expensive to find the joint spectrum Λ in (V.2) exactly. However, the graph shifts $\mathbf{S}_k, 1 \leq k \leq d$, in some engineering applications are symmetric and their spectrum sets are known being contained in some intervals [5], [7], [39], [40]. For instance, the normalized Laplacian matrix on a simple graph is symmetric and its spectrum is contained in $[0, 2]$. In this section, we use the Chebyshev approximation of the function h^{-1} to select the filters in (IV.5) when spectrum of the symmetric graph shift $\mathbf{S}_k, 1 \leq k \leq d$, are contained in some known intervals.

Let $\mathbf{S}_1, ..., \mathbf{S}_d$ be symmetric commutative graph shifts such that their joint spectrum Λ in (V.2) is contained in $[\mathbf{a}, \mathbf{b}] = [a_1, b_1] \times \cdots \times [a_d, b_d]$,

$$\boldsymbol{\lambda}_i \in [\mathbf{a}, \mathbf{b}] \text{ for all } \boldsymbol{\lambda}_i \in \Lambda. \tag{V.12}$$

and h be a multivariate polynomial satisfying

$$h(\mathbf{t}) \neq 0 \ \text{ for all } \ \mathbf{t} \in [\mathbf{a}, \mathbf{b}]. \tag{V.13}$$

Define Chebyshev polynomials $T_k, k \geq 0$, by

$$T_k(s) = \begin{cases} 1 & \text{if } k = 0, \\ s & \text{if } k = 1, \\ 2sT_{k-1}(s) - T_{k-2}(s) & \text{if } k \geq 2, \end{cases} \tag{V.14}$$

and shifted multivariate Chebyshev polynomials $\bar{T}_{\mathbf{k}}, \mathbf{k} = (k_1, \ldots, k_d) \in \mathbb{Z}_+^d$, on $[\mathbf{a}, \mathbf{b}]$ by

$$\bar{T}_{\mathbf{k}}(\mathbf{t}) = \prod_{i=1}^d T_{k_i}\Big(\frac{2t_i - a_i - b_i}{b_i - a_i}\Big), \quad \mathbf{t} = (t_1, ..., t_d) \in [\mathbf{a}, \mathbf{b}].$$

By (V.13), $1/h$ is an analytic function on $[\mathbf{a}, \mathbf{b}]$, and hence it has Fourier expansion in term of shifted Chebyshev polynomials $\bar{T}_{\mathbf{k}}, \mathbf{k} \in \mathbb{Z}_+^d$,

$$\frac{1}{h(\mathbf{t})} = \sum_{\mathbf{k} \in \mathbb{Z}_+^d} c_{\mathbf{k}} \bar{T}_{\mathbf{k}}(\mathbf{t}), \ \mathbf{t} \in [\mathbf{a}, \mathbf{b}], \tag{V.15}$$

where

$$c_{\mathbf{k}} = \frac{2^{d-p(\mathbf{k})}}{\pi^d} \int_{[0,\pi]^d} \frac{\bar{T}_{\mathbf{k}}(t_1(\boldsymbol{\theta}), \ldots, t_d(\boldsymbol{\theta}))}{h(t_1(\boldsymbol{\theta}), \ldots, t_d(\boldsymbol{\theta}))} d\boldsymbol{\theta}, \ \mathbf{k} \in \mathbb{Z}_+^d, \tag{V.16}$$

$p(\mathbf{k})$ is the number of zero components in $\mathbf{k} \in \mathbb{Z}_+^d$, and $t_i(\boldsymbol{\theta}) = \frac{a_i+b_i}{2} + \frac{b_i-a_i}{2}\cos(\theta_i), 1 \leq i \leq d$, for $\boldsymbol{\theta} = (\theta_1, ..., \theta_d)$. Define partial sum of the expansion (V.15) by

$$g_K(\mathbf{t}) = \sum_{|\mathbf{k}| \leq K} c_{\mathbf{k}} \bar{T}_{\mathbf{k}}(\mathbf{t}), \ K \geq 0. \tag{V.17}$$

Due to the analytic property of the polynomial h, the partial sum $g_K, K \geq 0$, converges to $1/h$ exponentially [41],

$$\max_{\mathbf{t} \in [\mathbf{a}, \mathbf{b}]} |1 - h(\mathbf{t})g_K(\mathbf{t})| \leq Cr_0^K, \ K \geq 0, \tag{V.18}$$

for some positive constants $C \in (0, \infty)$ and $r_0 \in (0, 1)$. Hence

$$\max_{\mathbf{t} \in [\mathbf{a}, \mathbf{b}]} |1 - h(\mathbf{t})g_K(\mathbf{t})| < 1 \tag{V.19}$$

for large K. Due to symmetry and commutativity of the graph shifts $\mathbf{S}_1, \ldots, \mathbf{S}_d$, they can be diagonalized simultaneously, and hence there exists an orthogonal matrix $\mathbf{U}$ such that $\mathbf{U}^T(\mathbf{I} - \mathbf{H}\mathbf{G}_K)\mathbf{U}$ is a diagonal matrix with diagonal entries $1 - h(\boldsymbol{\lambda}_i)g_K(\boldsymbol{\lambda}_i), 1 \leq i \leq N$, where $\boldsymbol{\lambda}_1, \ldots, \boldsymbol{\lambda}_N \in \Lambda$ and

$$\mathbf{G}_K = g_K(\mathbf{S}_1, \ldots, \mathbf{S}_d). \tag{V.20}$$

This implies that

$$b_K := \sup_{1 \leq i \leq N} |1 - h(\boldsymbol{\lambda}_i)g_K(\boldsymbol{\lambda}_i)| \leq Cr_0^K, \tag{V.21}$$

where the last inequality follows from (V.12) and (V.19). For the Chebyshev polynomial filter $\mathbf{G}_K$ in (V.20), we call the iterative approximation algorithm (IV.5) and (IV.6) with the graph filter $\mathbf{G}$ replaced by $\mathbf{G}_K$ by the *iterative Chebyshev polynomial approximation algorithm*, or ICPA in abbreviation,

$$\begin{cases} \mathbf{z}^{(m)} = \mathbf{G}_K \mathbf{b}^{(m-1)} \\ \mathbf{b}^{(m)} = \mathbf{b}^{(m-1)} - \mathbf{H}\mathbf{z}^{(m)} \\ \mathbf{x}^{(m)} = \mathbf{x}^{(m-1)} + \mathbf{z}^{(m)}, \ m \geq 1, \end{cases} \tag{V.22}$$

with initial given in (IV.6). Then it follows from (V.12), (V.21) and Theorem IV.1 that the ICPA algorithm (V.22) converges exponentially when the degree K is so chosen that (V.19) holds.

Theorem V.3. Let $\mathbf{S}_1, ..., \mathbf{S}_d$ be commutative graph shifts, $\mathbf{H}$ be a polynomial graph filter of the graph shifts, $\mathbf{b}$ be a graph signal, and let degree $K \geq 0$ of Chebyshev polynomial approximation be so chosen that (V.19) holds. Then $\mathbf{x}^{(m)}, m \geq 0$, in the ICPA algorithm (V.22) converges exponentially to $\mathbf{H}^{-1}\mathbf{b}$, and

$$\|\mathbf{x}^{(m)} - \mathbf{H}^{-1}\mathbf{b}\|_2 \leq \frac{\|\mathbf{H}\|_2\|\mathbf{G}\|_2}{1 - b_K}(b_K)^m\|\mathbf{H}^{-1}\mathbf{b}\|_2, \ m \geq 1.$$

By (V.18), an inverse filtering procedure (IV.1) can be approximately implemented by the filter procedure $\mathbf{G}_K\mathbf{x}$ with large K, i.e., $\mathbf{H}^{-1}\mathbf{x} \approx \mathbf{G}_K\mathbf{x}$ for large K. The above implementation of the inverse filtering has been discussed in [12], [26] for the case that $\mathbf{H}$ is a polynomial graph filter of one shift, and it is known as the Chebyshev polynomial approximation algorithm (CPA). By (IV.8), the approximation $\mathbf{G}_K\mathbf{x}$ in the CPA is the same as the first term $\mathbf{x}^{(1)}$ in the ICPA algorithm (V.22). To implement the inverse filtering with high accuracy, the CPA requires Chebyshev polynomial approximation of high degree, which means more integrals involved in coefficient calculations. On the other hand, we can select Chebyshev polynomial approximation of lower degree in the ICPA algorithm (V.22) to reach the same accuracy with

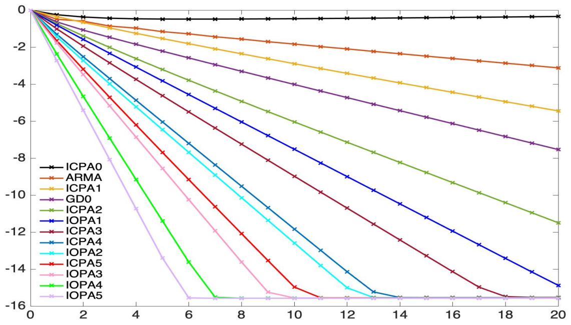

Fig. 5: Plotted are average of the relative iteration error $\log_{10}(AE(m)), 0 \le m \le 20$, in logarithmic scale of the IOPA algorithm, the ICPA algorithm, the GD0 algorithm and the ARMA algorithm. This confirms their exponential convergence, except the divergence of the ICPA algorithm with degree zero.

few iterations. Our simulation in the next section confirms that the above observation, see Table I.

VI. Simulations

In this section, we demonstrate the iterative optimal polynomial approximation (IOPA) algorithm (V.9) and the iterative Chebyshev polynomial approximation (ICPA) algorithm (V.22) to implement an inverse polynomial filtering procedure, and compare their performances with the gradient decent method with zero initial [25], and the autoregressive moving average (ARMA) algorithm [22]. We also apply our proposed algorithms for denoising time-varying signals governed by a differential equation and the data set of US hourly temperatures at 218 locations.

A. *Iterative approximation algorithms on circulant graphs*

Let $h_1(t) = (9/4-t)(3+t)$. In this subsection, we consider inverse filtering procedure corresponding to the polynomial filter $\mathbf{H}_1 = h_1(\mathbf{L}^{\rm sym})$ of the normalized Laplacian $\mathbf{L}^{\rm sym}$ on the circulant graph $\mathcal{C}$ with 50 nodes and generating set $S = \{1, 2, 5\}$, see Figure 1. As all eigenvalues of the normalized Lapalician $\mathbf{L}^{\rm sym}$ are contained in $[0, 2]$ and $h_1(t) \ne 0$ for all $0 \le t \le 2$, the optimal polynomial approximations $g_L^*, L \ge 0$ in (V.6) and the Chebyshev polynomial approximations $g_K, K \ge 0$, in (V.17) provide good approximations to $1/h_1$ on $[0, 2]$.

Let a_L^*, $L \ge 0$ and b_K, $K \ge 0$, be as in (V.10) and (V.21) respectively. Our numerical calculation shows that $a_L^*, 0 \le L \le 5$, are given by 0.4501, 0.1850, 0.0608, $0.0210, 0.0060, 0.0023$, and that $b_K, 0 \le K \le 5$, are given by 1.0463, $0.5837, 0.2880, 0.1431, 0.0719, 0.0367$ respectively. Therefore, the IOPA algorithm (V.9) for $0 \le L \le 5$, IOPAL in abbreviation, converges with convergence rate a_L^* by Theorem V.1, and similarly the ICPA algorithm (V.22) for $1 \le K \le 5$, ICPAK in abbreviation, converges with convergence rate b_K by Theorem V.3. Hence those two algorithms are applicable for the inverse filtering procedure $\mathbf{b} \longmapsto \mathbf{H}_1^{-1}\mathbf{b}$. Shown in Table I and Figure 5 are the simulation results, where the original input signal $\mathbf{x}$ has entries randomly selected in $[-1, 1]$, the observation is $\mathbf{b} = \mathbf{H}_1\mathbf{x}$, and $AE(m), m \ge 1$, are the average of the relative iteration error $E(m, \mathbf{x})$ over 1000 trials,

$$E(m, \mathbf{x}) = \|\mathbf{x}^{(m)} - \mathbf{x}\|_2/\|\mathbf{x}\|_2,\ m \ge 1,$$

and $\mathbf{x}^{(m)}, m \ge 1$, are the output at m-th iteration of the iterative algorithm. Both Table I and Figure 5 confirm the exponential convergence and applicability of inverse filtering procedure of the IOPAL, $0 \le L \le 5$ and ICPAK, $1 \le K \le 5$. From Table I, we observe that the IOPAL algorithms with higher degree L (resp. the ICPAK with higher degree K) have faster convergence, and the IOPAL algorithm outperforms the ICPAK algorithm when the same degree $L = K$ is selected. As $b_0 > 1$, the ICPA algorithm (V.22) with $K = 0$ does not yield the desired inverse filtering procedure, see the black line in Figure 5 and the third column in Table I.

The filter $\mathbf{H}_1$ is positive definitive with minimal and maximal eigenvalues being 2.56 and 6.75 respectively. The gradient descent method with zero initial, GD0 in abbreviation, and step length parameter $\gamma \in (0, 2/6.75)$ can be applied for the inverse filtering. As mentioned in Remarks IV.2 and V.2, we will use the optimal step length $\gamma = 2/(6.75 + 2.56)$ in our simulations, and then the gradient descent method with zero initial is the same as the IOPA algorithm (V.9) with $L = 0$, i.e., GD0=IOPA0. As

$$\frac{1}{h_1(t)} = \frac{4/21}{9/4-t} + \frac{4/21}{3+t},$$

the requirement (IV.12) for the ARMA is satisfied and hence the ARMA method can be used in the inverse filtering procedure corresponding to the polynomial filter $\mathbf{H}_1 = h_1(\mathbf{L}^{\rm sym})$. Shown in Table I and Figure 5 are the simulation results to apply the GD0 algorithm and ARMA method for the inverse filtering procedure $\mathbf{b} \longmapsto \mathbf{H}_1^{-1}\mathbf{b}$. Comparing with the ARMA algorithm and the GD0 algorithm, we observe that the proposed IOPAL algorithms with $L \ge 1$ and ICPAK algorithms with $K \ge 2$ have faster convergence, while the GD0 algorithm outperforms the ICPAK when $K = 1$.

B. *Denoising time-varying signals*

Graph signal denoising is one of the most popular applications in graph filtering [8]–[11], [14], [15], [17], [18], [22]. In this subsection, we consider denoising noisy sampling data

$$\mathbf{b}_i = \mathbf{x}(t_i) + \boldsymbol{\eta}_i,\ 1 \le i \le M, \tag{VI.1}$$

of some time-varying signal $\mathbf{x}(t)$ on a undirected graph $\mathcal{G}$ governed by a differential equation

$$\mathbf{x}''(t) = \mathbf{P}\mathbf{x}(t), \tag{VI.2}$$

where $\boldsymbol{\eta}_i, 1 \le i \le M$, are noises with noise level $\eta = \max_{1\le i\le M} \|\boldsymbol{\eta}_i\|_\infty$, the sampling procedure are taken uniformly at $t_i = t_1 + (i-1)\delta, 1 \le i \le M$, with uniform sampling gap $\delta > 0$, and $\mathbf{P}$ is a graph filter on the graph $\mathcal{G}$ with small bandwidth. Presented in Figure 6 are two snapshots of a time-varying graph signal in (VI.2) on the random geometric graph $\mathcal{G}_{512}$ reproduced by the GSPToolbox, which has 512 vertices randomly deployed in the region $[0, 1]^2$ and an edge existing between two vertices if their physical distance is not larger than $\sqrt{2/512} = 1/16$ [14], [43].

Discretizing the differential equation (VI.2) gives

TABLE I: Average relative iteration error in 1000 trials for the ARMA algorithm, the gradient decent algorithm with zero initial, and the IOPA and ICPA algorithms with different degrees.

AE Alg. m	ARMA	GD0	ICPA0	IOPA1	ICPA1	IOPA2	ICPA2	IOPA3	ICPA3	IOPA4	ICPA4	IOPA5	ICPA5
1	0.3230	0.2329	0.5676	0.1544	0.4491	0.0362	0.1855	0.0168	0.0977	0.0043	0.0498	0.0019	0.0224
2	0.2551	0.0841	0.4278	0.0265	0.2187	0.0019	0.0410	0.0003	0.0114	0.0000	0.0031	0.0000	0.0006
3	0.1392	0.0341	0.3678	0.0047	0.1099	0.0001	0.0097	0.0000	0.0014	0.0000	0.0002	0.0000	0.0000
4	0.1070	0.0143	0.3419	0.0008	0.0563	0.0000	0.0024	0.0000	0.0002	0.0000	0.0000	0.0000	0.0000
5	0.0695	0.0061	0.3317	0.0002	0.0293	0.0000	0.0006	0.0000	0.0000	0.0000	0.0000	0.0000	0.0000
7	0.0367	0.0011	0.3303	0.0000	0.0082	0.0000	0.0000	0.0000	0.0000	0.0000	0.0000	0.0000	0.0000
9	0.0198	0.0002	0.3391	0.0000	0.0024	0.0000	0.0000	0.0000	0.0000	0.0000	0.0000	0.0000	0.0000
11	0.0108	0.0000	0.3529	0.0000	0.0007	0.0000	0.0000	0.0000	0.0000	0.0000	0.0000	0.0000	0.0000
14	0.0044	0.0000	0.3800	0.0000	0.0001	0.0000	0.0000	0.0000	0.0000	0.0000	0.0000	0.0000	0.0000
17	0.0018	0.0000	0.4139	0.0000	0.0000	0.0000	0.0000	0.0000	0.0000	0.0000	0.0000	0.0000	0.0000
20	0.0008	0.0000	0.4543	0.0000	0.0000	0.0000	0.0000	0.0000	0.0000	0.0000	0.0000	0.0000	0.0000

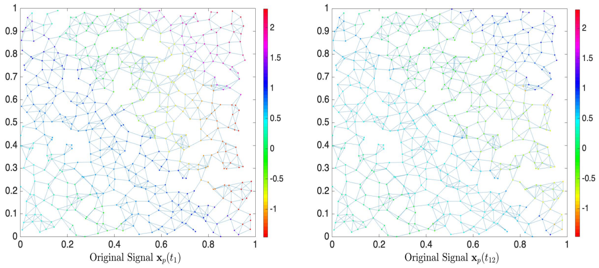

Fig. 6: Presented on the left and right are the first snapshot $\mathbf{x}_p(t_1)$ and the middle snapshot $\mathbf{x}_p(t_{12})$ of a time-varying signal $\mathbf{x}_p(t_i), 1 \le i \le M$, on the random geometric graph $\mathcal{G}_{512}$ respectively, where $M = 24$, $\delta = 0.1$, $t_i = (i-1)\delta$ for $1 \le i \le M$, $\mathbf{L}^{\rm sym}_{\mathcal{G}_{512}}$ is the normalized Lapalcian matrix on $\mathcal{G}_{512}$, the governing filter in the differential equation (VI.2) is given by $\mathbf{P} = -\mathbf{I} + \mathbf{L}^{\rm sym}_{\mathcal{G}_{512}}/2$, and the initial graph signal $\mathbf{x}_p(t_1)$ is a blockwise polynomial consisting of four strips and imposing $(0.5 - 2i_x)$ on the first and third diagonal strips and $(0.5 + i_x^2 + i_y^2)$ on the second and fourth strips respectively, where (i_x, i_y) are the coordinates of vertices [14].

$$\delta^{-2}\big(\mathbf{x}(t_{i+1}) + \mathbf{x}(t_{i-1}) - 2\mathbf{x}(t_i)\big) \approx \mathbf{P}\mathbf{x}(t_i), \qquad \text{(VI.3)}$$

where $i = 1, \ldots, M$. Applying the trivial extension $\mathbf{x}(t_0) = \mathbf{x}(t_1)$ and $\mathbf{x}(t_{M+1}) = \mathbf{x}(t_M)$ around the boundary, we can reformulate (VI.3) in a recurrence relation,

$$\mathbf{x}(t_i) \approx (2\mathbf{I} + \delta^2\mathbf{P})\mathbf{x}(t_{i-1}) - \mathbf{x}(t_{i-2}), 2 \le i \le M, \qquad \text{(VI.4)}$$

with $\mathbf{x}(t_0) = \mathbf{x}(t_1)$, or in the matrix form

$$(\delta^{-2}\mathbf{L}_{\mathcal{T}} \otimes \mathbf{I} + \mathbf{I} \otimes \mathbf{P})\mathbf{X} \approx \mathbf{0}, \qquad \text{(VI.5)}$$

where $\mathbf{L}_{\mathcal{T}}$ is the Laplacian matrix of the line graph $\mathcal{T}$ with vertices $\{t_1, \ldots, t_M\}$, and $\mathbf{X}$ is the vectorization of $\mathbf{x}(t_1), \ldots, \mathbf{x}(t_M)$.

In most of applications [11], [29], [35], [36], the time-varying signal $\mathbf{x}(t)$ at every moment t has certain smoothness in the vertex domain, which is usually described by

$$(\mathbf{x}(t_i))^T \mathbf{L}^{\rm sym}_{\mathcal{G}} \mathbf{x}(t_i) \approx 0, \ \ 1 \le i \le M. \qquad \text{(VI.6)}$$

For the time-varying signal $\mathbf{x}_p(t_i), 1 \le i \le 24$, in Figure 6. its average energy $(\sum_{i=1}^{24} \|\mathbf{x}_p(t_i))\|_2^2)/24$ is 221.2633, while the qualities $(\mathbf{x}_p(t_1))^T \mathbf{L}^{\rm sym}_{\mathcal{G}_{512}} \mathbf{x}_p(t_1), (\mathbf{x}_p(t_{12}))^T \mathbf{L}^{\rm sym}_{\mathcal{G}_{512}} \mathbf{x}_p(t_{12})$ and $\sum_{i=1}^{24} (\mathbf{x}_p(t_i))^T \mathbf{L}^{\rm sym}_{\mathcal{G}_{512}} \mathbf{x}_p(t_i)/24$ to measure smoothness of $\mathbf{x}_p(t_1)$ and $\mathbf{x}_p(t_{12})$ in the vertex domain and average smoothness of the time-varying signal $\mathbf{x}_p(t_i), 1 \le i \le 24$, are $84.1992, 42.4746$ and 43.1208 respectively. This indicates that the time-varying signal in Figure 6 has different smoothness at different moments.

Based on (VI.5) and (VI.6), we propose the following Tikhonov regularization approach,

$$\widehat{\mathbf{X}} := \arg\min_{\mathbf{Y}} \|\mathbf{Y} - \mathbf{B}\|_2^2 + \alpha \mathbf{Y}^T (\mathbf{I} \otimes \mathbf{L}^{\rm sym}_{\mathcal{G}}) \mathbf{Y}$$
$$+ \beta \mathbf{Y}^T (\delta^{-2}\mathbf{L}_{\mathcal{T}} \otimes \mathbf{I} + \mathbf{I} \otimes \mathbf{P}) \mathbf{Y}, \qquad \text{(VI.7)}$$

where $\mathbf{B}$ is the vectorization of the observed noisy sampling data $\mathbf{b}_1, \ldots, \mathbf{b}_M$, and α, β are penalty constants in the vertex and "temporal" domains chosen appropriately [23]. Set $\mathbf{H}_{\alpha,\beta} = \mathbf{I} + \alpha \mathbf{I} \otimes \mathbf{L}^{\rm sym}_{\mathcal{G}} + \beta(\delta^{-2}\mathbf{L}_{\mathcal{T}} \otimes \mathbf{I} + \mathbf{I} \otimes \mathbf{P}), \ \alpha, \beta \ge 0.$ The minimization problem (VI.7) has an explicit solution

$$\widehat{\mathbf{X}} = \mathbf{H}_{\alpha,\beta}^{-1} \mathbf{B}, \qquad \text{(VI.8)}$$

when $\mathbf{I} + \alpha \mathbf{L}^{\rm sym}_{\mathcal{G}} + \beta \mathbf{P}$ is positive definite. Set $\mathbf{S}_1 = \mathbf{I} \otimes \mathbf{L}^{\rm sym}_{\mathcal{G}}$ and $\mathbf{S}_2 = \frac{1}{2}\mathbf{L}_{\mathcal{T}} \otimes \mathbf{I}$. One may verify that $\mathbf{S}_1$ and $\mathbf{S}_2$ are commutative graph shifts on the Cartesian product graph $\mathcal{T} \times \mathcal{G}$ with their joint spectrum being contained in $[0, 2]^2$. Therefore for the case that $\mathbf{P} = p(\mathbf{L}^{\rm sym}_{\mathcal{G}})$ for some polynomial p, $\mathbf{H}_{\alpha,\beta} = h_{\alpha,\beta}(\mathbf{S}_1, \mathbf{S}_2)$ is a polynomial graph filter, where

$$h_{\alpha,\beta}(t_1, t_2) = 1 + \alpha t_1 + \beta p(t_1) + 2\beta\delta^{-2} t_2, \ \ 0 \le t_1, t_2 \le 2.$$

Hence we may use the IOPA algorithm (V.9) and the ICPA algorithm (V.22) to implement the denosing procedure (VI.8), where the polynomial filter $\mathbf{H}$ is replaced by $\mathbf{H}_{\alpha,\beta}$. Appropriate selection of the penalty constants α, β in the vertex and temporal domains are crucial to have a satisfactory denoising performance. In the simulations, we let noise entries of $\boldsymbol{\eta}_i, 1 \le i \le 24$ in (VI.2) be i.i.d. variables uniformly selected in the range $[-\eta, \eta]$, and we take

$$\alpha = \frac{\mathbb{E}\|\mathbf{B} - \mathbf{X}\|_2^2}{\mathbb{E}\big(\mathbf{B}^T (\mathbf{I} \otimes \mathbf{L}^{\rm sym}_{\mathcal{G}_{512}}) \mathbf{B}\big)} = \frac{MN\eta^2/3}{\mathbf{X}^T (\mathbf{I} \otimes \mathbf{L}^{\rm sym}_{\mathcal{G}_{512}}) \mathbf{X} + MN\eta^2/3}$$
$$\approx \frac{\eta^2}{0.2306 + \eta^2}, \qquad \text{(VI.9)}$$

and

$$\beta = \frac{\mathbb{E}\|\mathbf{B} - \mathbf{X}\|_2^2}{2\mathbb{E}\big(\mathbf{B}^T (\delta^{-2}\mathbf{L}_{\mathcal{T}} \otimes \mathbf{I} + \mathbf{I} \otimes \mathbf{P}) \mathbf{B}\big)}$$
$$= \frac{NM}{2\mathrm{tr}(\delta^{-2}\mathbf{L}_{\mathcal{T}} \otimes \mathbf{I} + \mathbf{I} \otimes \mathbf{P})} \approx 0.0026 \qquad \text{(VI.10)}$$

TABLE II: The average over 1000 trials of the signal-to-noise ratio $\mathrm{SNR}(m), m = 1, 2, 4, 6, \infty$ for noise level $\eta = 3/4, 1/2, 1/4, 1/8$, where penalty constants α and β are given in (VI.9) and (VI.10) respectively.

SNR m Alg.	1	2	4	6	∞
η=3/4, ISNR= 3.6274					
IOPA1(α, 0)	6.7609	6.9781	6.9671	6.9670	6.9670
IOPA1(0, β)	6.2978	6.3311	6.3142	6.3141	6.3141
IOPA1(α, β)	7.6595	8.6942	8.6580	8.6570	8.6569
ICPA1(α, 0)	6.6461	6.9894	6.9672	6.9670	6.9670
ICPA1(0, β)	6.2825	6.3303	6.3142	6.3141	6.3141
ICPA1(α, β)	7.5681	8.6240	8.6563	8.6569	8.6569
GD0(α, 0)	5.0952	6.8966	6.9795	6.9685	6.9670
GD0(0, β)	5.1637	6.6145	6.3625	6.3193	6.3141
GD0(α, β)	4.2726	7.1443	8.5091	8.6396	8.6569
η=1/2, ISNR=7.1480					
IOPA1(α, 0)	9.3943	9.5197	9.5169	9.5169	9.5169
IOPA1(0, β)	9.7314	9.8502	9.8337	9.8336	9.8336
IOPA1(α, β)	10.2225	11.2298	11.2250	11.2247	11.2247
ICPA1(α, 0)	9.3296	9.5233	9.5169	9.5169	9.5169
ICPA1(0, β)	9.7387	9.8496	9.8337	9.8336	9.8336
ICPA1(α, β)	9.8907	11.1739	11.2240	11.2246	11.2247
GD0(α, 0)	7.3466	9.3864	9.5191	9.5171	9.5169
GD0(0, β)	6.9938	9.8099	9.8773	9.8386	9.8336
GD0(α, β)	5.4263	9.1457	11.0489	11.2062	11.2247
η=1/4, ISNR= 13.1685					
IOPA1(α, 0)	14.0848	14.1030	14.1030	14.1030	14.1030
IOPA1(0, β)	15.3136	15.8658	15.8515	15.8515	15.8515
IOPA1(α, β)	14.8425	16.1266	16.1330	16.1329	16.1329
ICPA1(α, 0)	14.0719	14.1032	14.1030	14.1030	14.1030
ICPA1(0, β)	15.4306	15.8661	15.8515	15.8515	15.8515
ICPA1(α, β)	14.3528	16.0919	16.1327	16.1329	16.1329
GD0(α, 0)	12.4899	14.0724	14.1030	14.1030	14.1030
GD0(0, β)	8.6356	14.4052	15.8705	15.8560	15.8515
GD0(α, β)	7.3838	12.9623	15.9498	16.1189	16.1329
η=1/8, ISNR=19.1897					
IOPA1(α, 0)	19.4619	19.4629	19.4629	19.4629	19.4629
IOPA1(0, β)	19.9227	21.8660	21.8606	21.8605	21.8605
IOPA1(α, β)	19.3239	21.8422	21.8734	21.8735	21.8735
ICPA1(α, 0)	19.4609	19.4629	19.4629	19.4629	19.4629
ICPA1(0, β)	20.3403	21.8700	21.8606	21.8605	21.8605
ICPA1(α, β)	19.1871	21.8329	21.8734	21.8735	21.8735
GD0(α, 0)	18.7944	19.4613	19.4629	19.4629	19.4629
GD0(0, β)	9.1653	17.1639	21.7825	21.8629	21.8605
GD0(α, β)	8.6762	16.2445	21.5802	21.8550	21.8735

to balance three quantities in (VI.7) on noises and penalties on the vertex and temporal domains.

Denote the IOPA algorithm (V.9) with $L = 1$, the ICPA algorithm (V.22) with $K = 1$ and the gradient descent method (I.6) with zero initial to implement the inverse filter procedure $\mathbf{B} \longmapsto \widehat{\mathbf{X}} = \mathbf{H}_{\alpha,\beta}^{-1}\mathbf{B}$ by IOPA1(α, β), ICPA1(α, β) and GD0(α, β) respectively. Let $\widehat{\mathbf{X}}^{(m)}, m \geq 1$, be the outputs of either the IOPA1(α, β) algorithm, or the ICPA1(α, β) algorithm, or the GD0(α, β) method at m-th iteration. Due to the exponential convergence property of $\widehat{\mathbf{X}}^{(m)}, m \geq 1$, we may also use $\widehat{\mathbf{X}}^{(m)}$ with large m as a denoised time-varying signal.

To measure the denoising performance of our approaches, we define the input signal-to-noise ratio

$$\mathrm{ISNR} = -20 \log_{10} \frac{\|\mathbf{B} - \mathbf{X}\|_2}{\|\mathbf{X}\|_2},$$

and the output signal-to-noise ratio

$$\mathrm{SNR}(m) = -20 \log_{10} \frac{\|\widehat{\mathbf{X}}^{(m)} - \mathbf{X}\|_2}{\|\mathbf{X}\|_2},\ m \geq 1,$$

and

$$\mathrm{SNR}(\infty) = -20 \log_{10} \frac{\|\widehat{\mathbf{X}} - \mathbf{X}\|_2}{\|\mathbf{X}\|_2}.$$

Presented in Table II are the average over 1000 trials of the input signal-to-noise ratio ISNR and the output signal-to-noise ratio $\mathrm{SNR}(m), m = 1, 2, 4, 6, \infty$, where $M = 24, N = 512$ and $\mathbf{X}$ is the vectorization of the time-varying signal $\mathbf{x}_p(t_i), 1 \leq i \leq 24$ in Figure 6. From Table II, we observe that the denoising procedure $\mathbf{B} \longmapsto \widehat{\mathbf{X}} = \mathbf{H}_{\alpha,\beta}^{-1}\mathbf{B}$ via Tikhonov regularization (VI.7) on the temporal-vertex domain can improve the signal-to-noise ratio in the range from 2 to 5dBs, depending on the noise level η, and the denoising procedure $\mathbf{B} \longmapsto \widehat{\mathbf{X}}^{(m)}$ via the output of the m-th iteration in IOPA1(α, β) algorithm with $m \geq 2$, the GD0(α, β) method and the ICPA1(α, β) algorithm with $m \geq 4$ have similar denoising performance. Due to the correlation of time-varying signals across the joint vertex and temporal domains, it is expected that the Tikhonov regularization (VI.7) on the temporal-vertex domain has better denoising performance than Tikhonov regularizationd on the vertex domain (i.e., $\beta = 0$ in (VI.7)) and the temporal domain (i.e., $\alpha = 0$ in (VI.7)) do. The above performance expectation is confirmed in Table II. We remark that denoising approach via the Tikhonov regularization on the temporal-vertex domain is an inverse filtering procedure of a polynomial graph filter of *two* shifts, while the one on the vertex/temporal domain is an inverse filtering procedure of a polynomial graph filter of *one* shift.

C. Denoising an hourly temperature data set

In the subsection, we consider denoising the hourly temperature data set collected at 218 locations in the United States on August 1st, 2010 [42]. The above real-world data set is of size 218×24, and it can be modelled as a time-varying signal $\mathbf{w}(i), 1 \leq i \leq 24$, on the product graph $\mathcal{C} \times \mathcal{W}$, where $\mathcal{C}$ is the cycle graph with 24 vertices and generator $\{1\}$ and $\mathcal{W}$ is the undirected graph with 218 locations as vertices and edges constructed by the 5 nearest neighboring algorithm, see Figure 8 for two snapshots of the data set.

Given noisy temperature data

$$\widetilde{\mathbf{w}}_i = \mathbf{w}_i + \boldsymbol{\eta}_i,\ i = 1, \ldots, 24, \tag{VI.11}$$

we propose the following denosing approach,

$$\widehat{\mathbf{W}} := \arg\min_{\mathbf{Z}} \|\mathbf{Z} - \widetilde{\mathbf{W}}\|_2^2 + \tilde{\alpha}\mathbf{Z}^T(\mathbf{I} \otimes \mathbf{L}_{\mathcal{W}}^{\mathrm{sym}})\mathbf{Z} + \tilde{\beta}\mathbf{Z}^T(\mathbf{L}_{\mathcal{C}}^{\mathrm{sym}} \otimes \mathbf{I})\mathbf{Z}, \tag{VI.12}$$

where $\widetilde{\mathbf{W}}$ is the vectorization of the noisy temperature data $\widetilde{\mathbf{w}}_1, \ldots, \widetilde{\mathbf{w}}_{24}$ with noises $\boldsymbol{\eta}_i, 1 \leq i \leq 24$ in (VI.2) having their components randomly selected in $[-\eta, \eta]$ in a uniform distribution, $\mathbf{L}_{\mathcal{W}}^{\mathrm{sym}}$ and $\mathbf{L}_{\mathcal{C}}^{\mathrm{sym}}$ are normalized Laplacian matrices on the graph $\mathcal{W}$ and $\mathcal{C}$ respectively, and $\tilde{\alpha}, \tilde{\beta} \geq 0$ are penalty constants in the vertex and temporal domains chosen appropriately.

Set $\tilde{\mathbf{S}}_1 = \mathbf{I} \otimes \mathbf{L}_{\mathcal{W}}^{\mathrm{sym}}$, $\tilde{\mathbf{S}}_2 = \mathbf{L}_{\mathcal{C}}^{\mathrm{sym}} \otimes \mathbf{I}$ and $\mathbf{F}_{\tilde{\alpha},\tilde{\beta}} = \mathbf{I} + \tilde{\alpha}\tilde{\mathbf{S}}_1 + \tilde{\beta}\tilde{\mathbf{S}}_2,\ \tilde{\alpha}, \tilde{\beta} \geq 0$. One may verify that the explicit solution of the minimization problem (VI.12) is given by $\widehat{\mathbf{W}} = (\mathbf{F}_{\tilde{\alpha},\tilde{\beta}})^{-1}\widetilde{\mathbf{W}}$, and the proposed approach to denoise the temperature data set

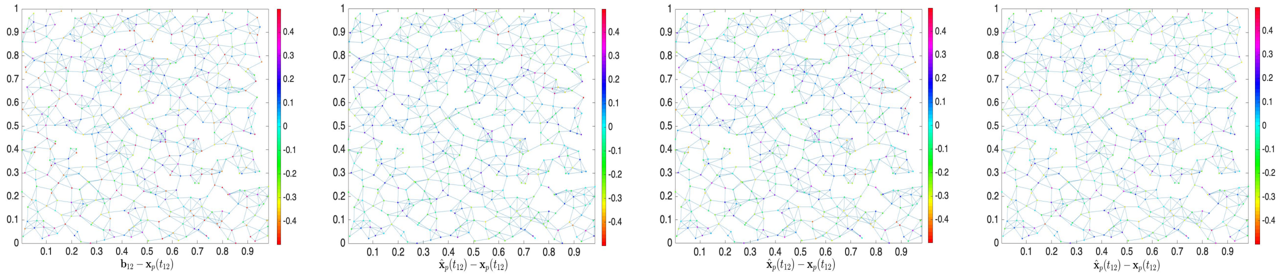

Fig. 7: Plotted on the left is the difference $\mathbf{b}_{12} - \mathbf{x}_p(t_{12})$ between the middle snapshot $\mathbf{x}_p(t_{12})$ in Figure 6 and its noisy data $\mathbf{b}_{12}$ with noise level $\eta = 1/2$. The energy $\|\mathbf{b}_{12} - \mathbf{x}_p(t_{12})\|_2^2$ is 41.8089. Plotted from the second to the fourth figures are the difference $\hat{\mathbf{x}}_p(t_{12}) - \mathbf{x}_p(t_{12})$ between $\mathbf{x}_p(t_{12})$ and $\hat{\mathbf{x}}_p(t_{12})$ of the denoised time-varying signals $\mathbf{H}_{\alpha,\beta}^{-1}\mathbf{B}, \mathbf{H}_{\alpha,0}^{-1}\mathbf{B}$ and $\mathbf{H}_{0,\beta}^{-1}\mathbf{B}$ respectively. The energy $\|\hat{\mathbf{x}}_p(t_{12}) - \mathbf{x}_p(t_{12})\|_2^2$ of those three are $16.2199, 24.3105, 22.1655$ respectively.

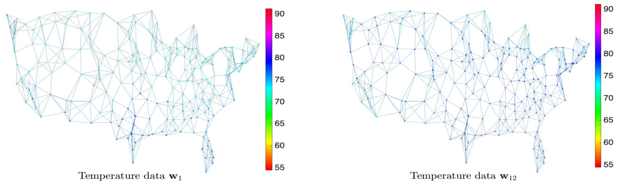
90
85
80
75
70
65
60
55
Temperature data $\mathbf{w}_1$
Temperature data $\mathbf{w}_{12}$

Fig. 8: Presented on the left and right sides are the temperature data $\mathbf{w}_1$ and $\mathbf{w}_{12}$, where $\mathbf{w}_i$, $1 \le i \le 24$, are the hourly temperature of 218 locations in the United States on August 1st, 2010.

becomes an inverse filtering procedure (IV.1) with $\mathbf{H}$ and $\mathbf{b}$ replaced by $\mathbf{F}_{\tilde\alpha,\tilde\beta}$ and $\widetilde{\mathbf{W}}$ respectively. In absence of notation, we still denote the IOPA algorithm (V.9) with $L = 1$, the ICPA algorithm (V.22) with $K = 1$ and the gradient descent method (I.6) with initial zero to implement the inverse filter procedure $\widetilde{\mathbf{W}} \longmapsto \mathbf{F}_{\tilde\alpha,\tilde\beta}^{-1}\widetilde{\mathbf{W}}$ by IOPA1$(\tilde\alpha, \tilde\beta)$, ICPA1$(\tilde\alpha, \tilde\beta)$ and GD0$(\tilde\alpha, \tilde\beta)$ respectively.

In our simulations, we take

$$\tilde\alpha = \frac{\mathbb{E}\|\mathbf{Z} - \widetilde{\mathbf{W}}\|_2^2}{\mathbb{E}\big(\widetilde{\mathbf{W}}^T\tilde{\mathbf{S}}_1\widetilde{\mathbf{W}}\big)} = \frac{4096\eta^2}{\mathbf{W}^T\tilde{\mathbf{S}}_1\mathbf{W} + 4096\eta^2},$$

and

$$\tilde\beta = \frac{\mathbb{E}\|\mathbf{Z} - \widetilde{\mathbf{W}}\|_2^2}{\mathbb{E}(\widetilde{\mathbf{W}}^T\tilde{\mathbf{S}}_2\widetilde{\mathbf{W}})} = \frac{4096\eta^2}{\mathbf{W}^T\tilde{\mathbf{S}}_2\mathbf{W} + 4096\eta^2}$$

to balance three terms in the regularization approach (VI.12). Presented in Table III are the average over 1000 trials of the input signal-to-noise ratio ISNR and the output signal-to-noise ratio

$$\mathrm{SNR}(m) = -20\log_{10}\frac{\|\widehat{\mathbf{W}}^{(m)} - \mathbf{W}\|_2}{\|\mathbf{W}\|_2},\ m \ge 1,$$

which are used to measure the denoising performance of the IOPA1$(\tilde\alpha, \tilde\beta)$, ICPA1$(\tilde\alpha, \tilde\beta)$ and GD0$(\tilde\alpha, \tilde\beta)$ at the mth iteration, where $\widehat{\mathbf{W}}^{(\infty)} := \widehat{\mathbf{W}}$ and $\widehat{\mathbf{W}}^{(m)}, m \ge 1$, are outputs of the IOPA1$(\tilde\alpha, \tilde\beta)$ algorithm, or the ICPA1$(\tilde\alpha, \tilde\beta)$, or the GD0$(\tilde\alpha, \tilde\beta)$ at m-th iteration. From Table III, we observe that the Tikhonov regularization on the temporal-vertex domain has better performance on denoising the hourly temperature data set than the Tikhonov regularization on the vertex/temporal domain does. Also we observe that the temporal correlation has larger influence than the vertex correlation for small noise corruption $\eta \le 10$, while the influence on the vertex correlation is more significant than the temporal correlation for the moderate and larger noise corruption.

VII. Conclusions

Polynomial graph filters of multiple shifts are preferable to denoise and extract features for multidimensional graph signals, such as video or time-varying signals. A sufficient condition is derived for a graph filter to be a polynomial of multiple shifts. Some Tikhonov regularization approaches on the temporal-vertex domain to denoise a time-varying signal can be reformulated as an inverse filtering procedure for a polynomial graph filter of two shifts on the temporal-vertex domain. To implement an inverse filtering directly, a centralized implementation may suffer from high computational burden as the inverse graph filter usually has full bandwidth. Two exponentially convergent iterative algorithms are introduced for the inverse filtering procedure of a polynomial graph filter, and each iteration of the proposed algorithms can be implemented in a distributed network where each vertex is equipped with systems for limited data storage, computation power and data exchanging facility to its adjacent vertices, and also in a centralized facility with linear complexity. The proposed iterative algorithms are demonstrated to implement the inverse filtering procedure effectively and to have satisfactory performance on denoising multidimensional graph signals. Future works will concentrate on the design methodology of polynomial graph filters and their inverses for certain spectral characteristic.

Appendix
Polynomial graph filters of commutative shifts

Let $\mathbf{S}_1, ..., \mathbf{S}_d$ be commutative graph shifts and Λ be their joint spectrum given in (V.2). If a graph filter $\mathbf{H}$ is a polynomial of $\mathbf{S}_1, ..., \mathbf{S}_d$, then it commutes with $\mathbf{S}_k, 1 \le k \le d$, i.e.,

$$\mathbf{H}\mathbf{S}_k = \mathbf{S}_k\mathbf{H},\ 1 \le k \le d. \tag{A.1}$$

For $d = 1$, it is shown in [6, Theorem 1] that any filter satisfying (A.1) is a polynomial filter if the graph shift has distinct eigenvalues. In this appendix, we show that the necessary condition (A.1) is also sufficient under the additional assumption that the joint eigenvalues $\boldsymbol{\lambda}_i, 1 \le i \le N$, in the joint spectrum Λ are distinct.

Theorem A.1. Let $\mathbf{S}_1, \dots, \mathbf{S}_d$ be commutative graph filters, and the joint spectrum Λ be as in (V.2). If all elements

TABLE III: The average over 1000 trials of the signal-to-noise ratio $\mathrm{SNR}(m), m = 1, 2, 4, 6, \infty$ denoise the US hourly temperature data set collected at 218 locations on August 1st, 2010, where $\eta = 35, 20, 10, 5$.

SNR \ m Alg.	1	2	4	6	∞
η=35, ISNR= 11.5499					
IOPA1($\tilde{\alpha}$, 0)	14.8961	16.2645	16.2514	16.2513	16.2513
IOPA1(0, $\tilde{\beta}$)	13.9772	14.3918	14.3767	14.3766	14.3766
IOPA1($\tilde{\alpha}$, $\tilde{\beta}$)	13.1461	17.9446	18.0861	18.0835	18.0834
ICPA1($\tilde{\alpha}$, 0)	14.2836	16.3142	16.2525	16.2513	16.2513
ICPA1(0, $\tilde{\beta}$)	14.0648	14.3921	14.3767	14.3766	14.3766
ICPA1($\tilde{\alpha}$, $\tilde{\beta}$)	11.4743	17.3842	18.0823	18.0835	18.0834
GD0($\tilde{\alpha}$, 0)	7.2431	13.2059	16.1727	16.2543	16.2513
GD0(0, $\tilde{\beta}$)	8.3162	13.3959	14.4044	14.3813	14.3766
GD0($\tilde{\alpha}$, $\tilde{\beta}$)	5.0571	9.9162	16.3697	17.9093	18.0834
η=20, ISNR= 16.4065					
IOPA1($\tilde{\alpha}$, 0)	18.3200	20.2427	20.2430	20.2430	20.2430
IOPA1(0, $\tilde{\beta}$)	18.0441	19.2351	19.2245	19.2245	19.2245
IOPA1($\tilde{\alpha}$, $\tilde{\beta}$)	14.9742	21.6052	21.9570	21.9562	21.9562
ICPA1($\tilde{\alpha}$, 0)	17.5726	20.2606	20.2434	20.2430	20.2430
ICPA1(0, $\tilde{\beta}$)	18.3209	19.2373	19.2245	19.2245	19.2245
ICPA1($\tilde{\alpha}$, $\tilde{\beta}$)	12.7808	20.7198	21.9527	21.9562	21.9562
GD0($\tilde{\alpha}$, 0)	8.4619	15.7776	20.1253	20.2427	20.2430
GD0(0, $\tilde{\beta}$)	8.9819	16.1791	19.2045	19.2281	19.2245
GD0($\tilde{\alpha}$, $\tilde{\beta}$)	5.5606	10.9775	19.2710	21.6872	21.9562
η=10, ISNR=22.4309					
IOPA1($\tilde{\alpha}$, 0)	23.3601	24.5548	24.5547	24.5547	24.5547
IOPA1(0, $\tilde{\beta}$)	21.8096	25.1979	25.2018	25.2018	25.2018
IOPA1($\tilde{\alpha}$, $\tilde{\beta}$)	17.9223	25.9271	26.2505	26.2504	26.2504
ICPA1($\tilde{\alpha}$, 0)	22.5756	24.5557	24.5547	24.5547	24.5547
ICPA1(0, $\tilde{\beta}$)	22.4923	25.2064	25.2018	25.2018	25.2018
ICPA1($\tilde{\alpha}$, $\tilde{\beta}$)	15.3648	25.1058	26.2492	26.2504	26.2504
GD0($\tilde{\alpha}$, 0)	11.7106	21.2319	24.5376	24.5548	24.5547
GD0(0, $\tilde{\beta}$)	9.3684	18.1036	25.0129	25.2028	25.2018
GD0($\tilde{\alpha}$, $\tilde{\beta}$)	6.7404	13.3494	23.6532	26.0938	26.2504
η=5, ISNR=28.4514					
IOPA1($\tilde{\alpha}$, 0)	29.0552	29.2071	29.2071	29.2071	29.2071
IOPA1(0, $\tilde{\beta}$)	24.4012	31.0219	31.0571	31.0571	31.0571
IOPA1($\tilde{\alpha}$, $\tilde{\beta}$)	21.9545	30.9963	31.1659	31.1659	31.1659
ICPA1($\tilde{\alpha}$, 0)	28.8453	29.2072	29.2071	29.2071	29.2071
ICPA1(0, $\tilde{\beta}$)	25.3869	31.0425	31.0571	31.0571	31.0571
ICPA1($\tilde{\alpha}$, $\tilde{\beta}$)	19.9363	30.6853	31.1658	31.1659	31.1659
GD0($\tilde{\alpha}$, 0)	18.4954	28.6452	29.2071	29.2071	29.2071
GD0(0, $\tilde{\beta}$)	9.9154	19.5959	30.5321	31.0531	31.0571
GD0($\tilde{\alpha}$, $\tilde{\beta}$)	8.5412	16.9557	29.4009	31.1194	31.1659

$\boldsymbol{\lambda}_i, 1 \le i \le N$, in the set Λ are distinct, then any graph filter $\mathbf{H}$ satisfying (A.1) is a polynomial of $\mathbf{S}_1, ..., \mathbf{S}_d$, i.e., $\mathbf{H} = h(\mathbf{S}_1, ..., \mathbf{S}_d)$ for some polynomial h.

Proof. Let $\mathbf{U}$ be the unitary matrix in (V.1), matrices $\hat{\mathbf{S}}_1, \ldots, \hat{\mathbf{S}}_d$ be as in (V.1), and $\hat{\mathbf{H}} = \mathbf{U}^*\mathbf{H}\mathbf{U} = (\hat{H}(i,j))_{1\le i,j\le N}$. By the assumption on the set Λ, there exist an interpolating polynomial h such that

$$h(\hat{S}_1(i,i), ..., \hat{S}_d(i,i)) = \hat{H}(i,i),\ 1 \le i \le N, \qquad \text{(A.2)}$$

see [38, Theorem 1 on p. 58]. Set

$$\mathbf{F} = \mathbf{U}^*\big(\mathbf{H} - h(\mathbf{S}_1, ..., \mathbf{S}_d)\big)\mathbf{U} = \hat{\mathbf{H}} - h(\hat{\mathbf{S}}_1, \ldots, \hat{\mathbf{S}}_d). \quad \text{(A.3)}$$

Then it suffices to prove that $\mathbf{F}$ is the zero matrix.

Write $\mathbf{F} = (F(i,j))_{1\le i,j\le N}$. By (A.1), we have that $\mathbf{F}\hat{\mathbf{S}}_k = \hat{\mathbf{S}}_k\mathbf{F}$ for all $1 \le k \le d$. This together with the upper triangular property for $\hat{\mathbf{S}}_k, 1 \le k \le d$, implies that

$$\sum_{l=1}^{j} F(i,l)\hat{S}_k(l,j) = \sum_{l=i}^{N} \hat{S}_k(i,l)F(l,j), 1 \le i,j \le N. \qquad \text{(A.4)}$$

By the assumption on Λ, we can find $1 \le k(i,j) \le d$ for any $1 \le i \ne j \le N$ such that

$$\hat{S}_{k(i,j)}(i,i) \ne \hat{S}_{k(i,j)}(j,j). \qquad \text{(A.5)}$$

Now we apply (A.4) and (A.5) to prove

$$F(i,j) = 0 \qquad \text{(A.6)}$$

by induction on $j = 1, \ldots, N$ and $i = N, \ldots, 1$.

For $i = N$ and $j = 1$, applying (A.4) with k replaced by $k(N,1)$, we obtain

$$F(N,1)\hat{S}_{k(N,1)}(1,1) = S_{k(N,1)}(N,N)F(N,1),$$

which together with (A.5) proves (A.6) for $(i,j) = (N,1)$. Inductively we assume that the conclusion (A.6) for all pairs (i,j) satisfying either $1 \le j \le j_0$ and $i = i_0$, or $1 \le j \le N$ and $i_0 < i \le N$.

For the case that $j_0 < i_0 - 1$, we have

$$\begin{aligned} & F(i_0, j_0+1)\hat{S}_{k(i_0,j_0+1)}(j_0+1, j_0+1) \\ = & \sum_{l=i_0}^{N} \hat{S}_{k(i_0,j_0+1)}(i_0, l)F(l, j_0+1) \\ = & \hat{S}_{k(i_0,j_0+1)}(i_0, i_0)F(i_0, j_0+1), \end{aligned}$$

where the second equality holds by the inductive hypothesis and the first equality is obtained from the inductive hypothesis and (A.4) with k replaced by $k(i_0, j_0+1)$. This together with (A.5) proves the conclusion (A.6) for $i = i_0$ and $j = j_0 + 1 \le i_0 - 1$, and hence the inductive proof can proceed for the case that $j_0 < i_0 - 1$.

For the case that the case that $j_0 = i_0 - 1$, it follows from the construction of the polynomial h and the upper triangular property for $\hat{\mathbf{S}}_k, 1 \le k \le d$, that the diagonal entries of $\mathbf{F}$ are

$$\hat{H}(i,i) - h(\hat{S}_1(i,i), ..., \hat{S}_d(i,i)) = 0, 1 \le i \le N$$

by (A.2). Hence the conclusion (A.6) holds for $i = i_0$ and $j = j_0 + 1$, and hence the inductive proof can proceed for the case that $j_0 = i_0 - 1$.

For the case that $i_0 \le j_0 \le N - 1$, we can follow the argument used in the proof for the case that $j_0 < i_0 - 1$ to establish the conclusion (A.6) for $i = i_0$ and $j = j_0 + 1 \le N$, and hence the inductive proof can proceed for the case that $i_0 \le j_0 \le N - 1$.

For the case that $j_0 = N$ and $i_0 \ge 2$, we obtain

$$\begin{aligned} & F(i_0 - 1, 1)\hat{S}_{k(i_0-1,1)}(1,1) \\ = & \sum_{l=i_0-1}^{N} \hat{S}_{k(i_0-1,l)}(i_0 - 1, l)F(l, 1) \\ = & \hat{S}_{k(i_0-1,1)}(i_0 - 1, i_0 - 1)F(i_0 - 1, 1), \end{aligned}$$

where the first equality follows from (A.4) with k replaced by $k(i_0 - 1, 1)$ and the second equality holds by the inductive hypothesis. This together with (A.5) proves the conclusion (A.6) for $i = i_0 - 1$ and $j = 1$, and hence the inductive proof can proceed for the case that $j_0 = N$ and $i_0 \ge 2$.

For the case that $j_0 = N$ and $i_0 = 1$, the inductive proof of the zero matrix property for the matrix $\mathbf{F}$ is complete. This completes the inductive proof. □

References

[1] D. I. Shuman, S. K. Narang, P. Frossard, A. Ortega, and P. Vandergheynst, “The emerging field of signal processing on graphs: Extending high-dimensional data analysis to networks and other irregular domains,” *IEEE Signal Process. Mag.*, vol. 30, no. 3, pp. 83-98, May 2013.

[2] A. Sandryhaila and J. M. F. Moura, “Big data analysis with signal processing on graphs: Representation and processing of massive data sets with irregular structure,” *IEEE Signal Process. Mag.*, vol. 31, no. 5, pp. 80-90, Sept. 2014.

[3] A. Ortega, P. Frossard, J. Kovačević, J. M. F. Moura, and P. Vandergheynst, “Graph signal processing: Overview, challenges, and applications,” *Proc. IEEE*, vol. 106, no. 5, pp. 808-828, May 2018.

[4] D. K. Hammod, P. Vandergheynst, and R. Gribonval, “Wavelets on graphs via spectral graph theory,” *Appl. Comput. Harmon. Anal.*, vol. 30, no. 4, pp. 129-150, Mar. 2011.

[5] S. K. Narang and A. Ortega, “Perfect reconstruction two-channel wavelet filter banks for graph structured data,” *IEEE Trans. Signal Process.*, vol. 60, no. 6, pp. 2786-2799, Jun. 2012.

[6] A. Sandryhaila and J. M. F. Moura, “Discrete signal processing on graphs,” *IEEE Trans. Signal Process.*, vol. 61, no. 7, pp. 1644-1656, Apr. 2013.

[7] O. Teke and P. P. Vaidyanathan, “Extending classical multirate signal processing theory to graphs Part II: M-channel filter banks,” *IEEE Trans. Signal Process.*, vol. 65, no. 2, pp. 423-437, Jan. 2017.

[8] A. Sandryhaila and J. M. F. Moura, “Discrete signal processing on graphs: Frequency analysis,” *IEEE Trans. Signal Process.*, vol. 62, no. 12, pp. 3042-3054, Jun. 2014.

[9] C. Cheng, Y. Jiang, and Q. Sun, “Spatially distributed sampling and reconstruction,” *Appl. Comput. Harmon. Anal.*, vol. 47, no. 1, pp. 109-148, Jul. 2019.

[10] J. Yi and L. Chai, “Graph filter design for multi-agent system consensus,” in *IEEE 56th Annual Conference on Decision and Control (CDC)*, Melbourne, VIC, 2017, pp. 1082-1087.

[11] W. Waheed and D. B. H. Tay, “Graph polynomial filter for signal denoising,” *IET Signal Process.*, vol. 12, no. 3, pp. 301-309, Apr. 2018.

[12] D. I. Shuman, P. Vandergheynst, D. Kressner, and P. Frossard, “Distributed signal processing via Chebyshev polynomial approximation,” *IEEE Trans. Signal Inf. Process. Netw.*, vol. 4, no. 4, pp. 736-751, Dec. 2018.

[13] E. Isufi, A. Loukas, N. Perraudin, and G. Leus, “Forecasting time series with VARMA recursions on graphs,” *IEEE Trans. Signal Process.*, vol. 67, no. 18, pp. 4870-4885, Sept. 2019.

[14] J. Jiang, C. Cheng, and Q. Sun, “Nonsubsampled graph filter banks: Theory and distributed algorithms,” *IEEE Trans. Signal Process.*, vol. 67, no. 15, pp. 3938-3953, Aug. 2019.

[15] M. Coutino, E. Isufi, and G. Leus, “Advances in distributed graph filtering,” *IEEE Trans. Signal Process.*, vol. 67, no. 9, pp. 2320-2333, May 2019.

[16] A. J. Laub, *Matrix Analysis for Scientists and Engineers*, PA, Philadelphia, SIAM, 2005.

[17] S. Segarra, A. G. Marques, and A. Ribeiro, “Optimal graph-filter design and applications to distributed linear network operators,” *IEEE Trans. Signal Process.*, vol. 65, no. 15, pp. 4117-4131, Aug. 2017.

[18] A. Gavili and X. Zhang, “On the shift operator, graph frequency, and optimal filtering in graph signal processing,” *IEEE Trans. Signal Process.*, vol. 65, no. 23, pp. 6303-6318, Dec. 2017.

[19] J. Jiang, D. B. Tay, Q. Sun, and S. Ouyang, “Design of nonsubsampled graph filter banks via lifting schemes,” *IEEE Signal Process. Lett.*, accepted, 2019.

[20] S. Chen, A. Sandryhaila, J. M. F. Moura, and J. Kovačević, “Signal recovery on graphs: variation minimization,” *IEEE Trans. Signal Process.*, vol. 63, no. 17, pp. 4609-4624, Sept. 2015.

[21] M. Onuki, S. Ono, M. Yamagishi, and Y. Tanaka, “Graph signal denoising via trilateral filter on graph spectral domain,” *IEEE Trans. Signal Inf. Process. Netw.*, vol. 2, no. 2, pp. 137-148, Jun. 2016.

[22] E. Isufi, A. Loukas, A. Simonetto, and G. Leus, “Autoregressive moving average graph filtering,” *IEEE Trans. Signal Process.*, vol. 65, no. 2, pp. 274-288, Jan. 2017.

[23] T. Kurokawa, T. Oki, and H. Nagao, “Multi-dimensional graph Fourier transform,” *arXiv*: 1712.07811, Dec. 2017.

[24] A. W. Bohannon, B. M. Sadler, and R. V. Balan, “A filtering framework for time-varying graph signals,” in *Vertex-Frequency Analysis of Graph Signals*, Springer, pp. 341-376, 2019.

[25] X. Shi, H. Feng, M. Zhai, T. Yang, and B. Hu, “Infinite impulse response graph filters in wireless sensor networks,” *IEEE Signal Process. Lett.*, vol. 22, no. 8, pp. 1113-1117, Aug. 2015.

[26] C. Cheng, J. Jiang, N. Emirov, and Q. Sun, “Iterative Chebyshev polynomial algorithm for signal denoising on graphs,” in *Proceeding 13th Int. Conf. on SampTA*, Bordeaux, France, Jul. 2019, sampta2019:267521.

[27] S. Chen, A. Sandryhaila, and J. Kovačević, “Distributed algorithm for graph signal inpainting,” *2015 IEEE International Conference on Acoustics, Speech and Signal Processing (ICASSP)*, Brisbane, QLD, 2015, pp. 3731-3735.

[28] K. Qiu, X. Mao, X. Shen, X. Wang, T. Li, and Y. Gu, “Time-varying graph signal reconstruction,” *IEEE J. Sel. Topics Signal Process.*, vol. 11, no. 6, pp. 870-883, Sept. 2017.

[29] V. N. Ekambaram, G. C. Fanti, B. Ayazifar, and K. Ramchandran, “Circulant structures and graph signal processing,” in *Proc. IEEE Int. Conf. Image Process.*, 2013, pp. 834-838.

[30] V. N. Ekambaram, G. C. Fanti, B. Ayazifar, and K. Ramchandran, “Multiresolution graph signal processing via circulant structures,” in *Proc. IEEE Digital Signal Process. Signal Process. Educ. Meeting (DSP/SPE)*, 2013, pp. 112-117.

[31] M. S. Kotzagiannidis and P. L. Dragotti, “Splines and wavelets on circulant graphs,” *Appl. Comput. Harmon. Anal.*, vol. 47, no. 2, pp. 481-515, Sept. 2019.

[32] M. S. Kotzagiannidis and P. L. Dragotti, “Sampling and reconstruction of sparse signals on circulant graphs – an introduction to graph-FRI,” *Appl. Comput. Harmon. Anal.*, vol. 47, no. 3, pp. 539-565, Nov. 2019.

[33] D. Valsesia, G. Fracastoro, and E. Magli, “Deep graph-convolutional image denoising,” *arXiv*:1907.08448, Jul. 2019.

[34] A. Loukas and D. Foucard, “Frequency analysis of time-varying graph signals,” in *IEEE Global Conf. Signal Inf. Process. (GlobalSIP)*, 2016, pp. 346-350.

[35] F. Grassi, A. Loukas, N. Perraudin, and B. Ricaud, “A time-vertex signal processing framework: scalable processing and meaningful representations for time-series on graphs,” *IEEE Trans. Signal Process.*, vol. 66, no. 3, pp. 817-829, Feb. 2018.

[36] R. A. Horn and C. R. Johnson. *Matrix Analysis*, Cambridge University Press, 2012.

[37] F. Chung and L. Lu, *Complex Graphs and Networks*, CBMS Regional Conference Series in Mathematics 107, Providence, RI, Amer Math. Soc., 2006.

[38] W. Cheney and W. Light. *A Course in Approximation Theory*, Brook/Cole Publishing Company, 2000.

[39] F. Chung, *Spectral Graph Theory*, CBMS Regional Conference Series in Mathematics, No. 92. Providence, RI, Amer. Math. Soc., 1997.

[40] A. Sakiyama, K. Watanabe, Y. Tanaka, and A. Ortega, “Two-channel critically sampled graph filter banks with spectral domain sampling,” *IEEE Trans. Signal Process.*, vol. 67, no. 6, pp. 1447-1460, Mar. 2019.

[41] G. M. Phillips, *Interpolation and Approximation by Polynomials*, CMS Books Math., Springer-Verlag, 2003.

[42] J. Zeng, G. Cheung, and A. Ortega, “Bipartite approximation for graph wavelet signal decomposition,” *IEEE Trans. Signal Process.*, vol. 65, no. 20, pp. 5466-5480, Oct. 2017.

[43] P. Nathanael, J. Paratte, D. Shuman, L. Martin, V. Kalofolias, P. Vandergheynst, and D. K. Hammond, “GSPBOX: A toolbox for signal processing on graphs,” *arXiv*:1408.5781, Aug. 2014.